PERGAMON

Planetary and Space Science 49 (2001) 3–22

Planetary and Space Science

www.elsevier.nl/locate/planspasci

Basic targeting strategies for rendezvous and flyby missions to the near-Earth asteroids

Ettore Perozzi[a,b,*], Alessandro Rossi[a,c], Giovanni B. Valsecchi[d]

[a] *DESPA-Observatoire de Paris Meudon, 5 Place Jules Janssen, 92195 Meudon, France*
[b] *Telespazio, Via Tiburtina 965, 00156 Roma, Italy*
[c] *Istituto CNUCE-CNR, Via S. Maria 36, 56126 Pisa, Italy*
[d] *I.A.S-CNR, Reparto di Planetologia, Area di Ricerca del C.N.R., via Fosso del Cavaliere 100, 00133 Roma, Italy*

Received 15 September 1999; received in revised form 22 June 2000; accepted 3 July 2000

Abstract

Missions to asteroids and comets are becoming increasingly feasible both from a technical and a financial point of view. In particular, those directed towards the Near-Earth Asteroids have proven suitable for a low-cost approach, thus attracting the major space agencies as well as private companies. The choice of a suitable target involves both scientific relevance and mission design considerations, being often a difficult task to accomplish due to the limited energy budget at disposal. The aim of this paper is to provide an approach to basic trajectory design which allows to account for both aspects of the problem, taking into account scientific and technical information. A global characterization of the Near-Earth Asteroids population carried out on the basis of their dynamics, physical properties and flight dynamics considerations, allows to identify a group of candidates which satisfy both, the scientific and engineering requirements. The feasibility of rendezvous and flyby missions towards them is then discussed and the possibility of repeated encounters with the same object is investigated, as an intermediate scenario. Within this framework, the capability of present and near future launch and propulsion systems for interplanetary missions is also addressed.

1. Introduction

In more than 30 years of planetary exploration, the experience gained in carrying out deep space missions has allowed to lower considerably their cost and their complexity. The success of the NASA Discovery program (e.g. Kicza and Vorder Bruegge, 1995) has pushed both international and national programs to endorse low-cost interplanetary mission studies of a scientific as well as of a technological character. The ESA SMART mission concept and the ambitious Japanese planetary exploration program witness the advances obtained so far.

Among the possible targets, the Near Earth Asteroids (NEAs), whose dynamical characteristics allow close approaches with our planet, are gaining an increasing importance in many respects: science, technology, and the commercial exploitation of space. These celestial bodies are scientifically relevant as dynamically and physically evolved primitive bodies of the solar system, technologically challenging for their possible future exploitation as extraterrestrial resources, while the recent issues devoted to protect our planet from cosmic impacts has brought them inside the broader topic of risk hazard assessment. Furthermore, from the point of view of mission analysis, their periodic proximity to our planet and the possibility of remaining well within the inner planetary region with the consequent advantages on thermal and electrical power requirements, allows to consider them as favourable targets for both, rendezvous and flyby missions. The NEAR mission (Farquhar, 1995), presently orbiting around 433 Eros, shows the actual feasibility of a highly sophisticated interplanetary mission with a first-class scientific target, at a reasonably low cost and spacecraft and operation complexity. On the other hand, the recently proposed NEAP mission by a private space enterprise (Benson, 1998), aimed to land on 4660 Nereus, shows that Near-Earth Asteroid are possibly to become the first targets for commercially available deep space missions.

When selecting the target for a space mission, one tries to maximize the ratio between its scientific return and its cost — the last parameter being, in the last decade, an increasingly important factor. Applying this simple

* Corresponding author. Tel.: +33-01-4507-7111; fax: +33-01-4507-7110.
E-mail address: perozzi@megasx.obspm.fr (E. Perozzi).

0032-0633/01/$ - see front matter
PII: S0032-0633(00)00124-0

criterion to NEAs, it appears that, with the notable exception of Eros — mainly due to its large dimensions and already visited by the aforementioned NEAR mission — the choice is rather open. Usually, the scientific community indicates a number of candidates solely on the basis of their scientific relevance, which must then be examined by the technical counterpart in order to check the feasibility of a mission, eventually undergoing cost estimates. It often happens that not only the "best choices" from a scientific point of view, but also the "intermediate ones" do not match safe engineering and management plans.

Some of the most frequent constraints influencing the target selection can be briefly summarized as: (a) rendezvous missions are obviously preferred allowing close and extended observations and measurements, but in general they are rather demanding in terms of energy requirements; (b) in spite of their periodic proximity to our planet most NEAs move on highly eccentric and/or inclined orbits, a fact that has nontrivial dynamical implications; (c) advanced propulsion systems, such as low-thrust electric propulsion, increase the overall energy budget of a mission but need longer periods of time to be fully exploited; (d) the spacecraft mass, the launch scenario and its timing, needed for Earth phasing, represent crucial parameters but are often defined rather late within the mission study.

In what follows, we have tried to give a comprehensive approach to the problem in order to provide a method which takes into consideration both, the scientific and the technical constraints. The possibility of defining quickly the accessibility of an object might prove especially useful when treating NEAs targeting, since only 20% of the population is presently known and with the recent operation of wide-field, high-sensitivity telescopes, the number of new discoveries is growing steadily with time.

After characterizing from a dynamical point of view the NEAs population and describing some basic flight dynamics tools, rendezvous missions are introduced. Through a comparison between the scientific relevance of each possible target and the corresponding estimate of the energy needed for a "best case" mission scenario, a subset of candidates is identified. These results are compared with the preferences expressed by the scientific community and the mission profiles developed for the ESA SMART-1 Asteroid Rendezvous Option (Barucci et al., 1998); although not selected (the mission is now aimed to the Moon) this study proved to be extremely useful in addressing the general topic of NEAs target selection. In fact, several high-priority targets for science, in particular the high- inclination ones, appeared definitely out of reach at the present technological level when considering basic rendezvous missions (i.e. no gravity-assisted trajectories are foreseen).

In order to increase the superposition among scientifically appealing targets and realistic mission profiles, flyby trajectories have been investigated too. In particular, the possibility of increasing the scientific return when using nodal resonant-flyby strategies is proposed. Finally, the results are discussed within the framework of launch and propulsion system scenarios.

2. The NEAs population

NEAs are generally believed to be dynamically evolved fragments of main-belt asteroids entering the inner solar system on chaotic orbits. Orbital resonances represent the leading mechanism for delivering matter from the main belt: thus most NEAs share the orbital paths of meteorites and their final fates, either colliding with a terrestrial planet, being ejected from the solar system on hyperbolic orbits, or melting into the Sun (Farinella et al., 1994). Yet a significant fraction of NEAs — up to 50% of the whole population (Binzel et al., 1992; Gladman et al., 1999) — might be composed by extinct cometary nuclei. The identification of a newly discovered NEA with periodic comet Wilson–Harrington, or of 3200 Phaeton as the parent-body of the Geminids meteor stream, are well-known examples of this kind.

Only a few "giant" NEAs exist (diameter larger than 10 km) and for them an ad hoc origin has been proposed (Zappalà et al., 1997); according to the available estimates, there should be about 1500 objects larger than 1 km, and about 150.000 are those larger than 100 m (Lupishko and Di Martino, 1998). A concentration of small objects (diameter less than 50 m) close to our planet has been proposed by Rabinowitz et al. (1993), with perihelia between 0.9 and 1.1 AU, and aphelia less than 1.4 AU.

The physical properties of NEAs may differ from those of main belt asteroids because of the consequences of the chaotic evolution of their orbits: close encounters with the planets may have distorted and disrupted weakly bound bodies (e.g. Richardson et al., 1998), while sun grazing passages resulted in strong thermal alteration processes (Farinella et al., 1994). Radar observations (e.g. Hudson et al., 1997) and the study of photometric lightcurves (Pravec et al., 1998a), have shown the occurrence of highly elongated shapes, binary systems (Pravec et al., 1998b), fast rotators, leading in some cases to extreme situations (Steel et al., 1997), and exotic rotation states (e.g. "tumbling", Ostro et al., 1995).

Although only about 10% of NEAs, as far as taxonomic classes are concerned (e.g. Gaffey et al., 1993), have been unambiguously classified, they show close similarities to main-belt asteroids and the corresponding meteorites. In particular, a few of them (M-type) seems to be of high metallic content, which is important for their possible exploitation, while C-type bodies would represent a sample of the pristine material characterizing the outer asteroid main belt. V-type asteroids are also interesting, because they are widely believed to be fragments of the basaltic surface of the large main belt asteroid 4 Vesta,

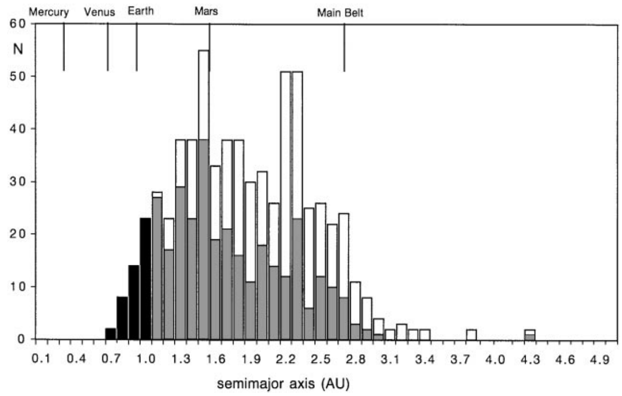

Fig. 1. Frequency histogram of NEAs semimajor axis. The cumulative number of objects within a given range (N) shows also the relative abundances: black refer to ATENs, gray to APOLLOs and white to AMORs. The bin size is 0.1 AU.

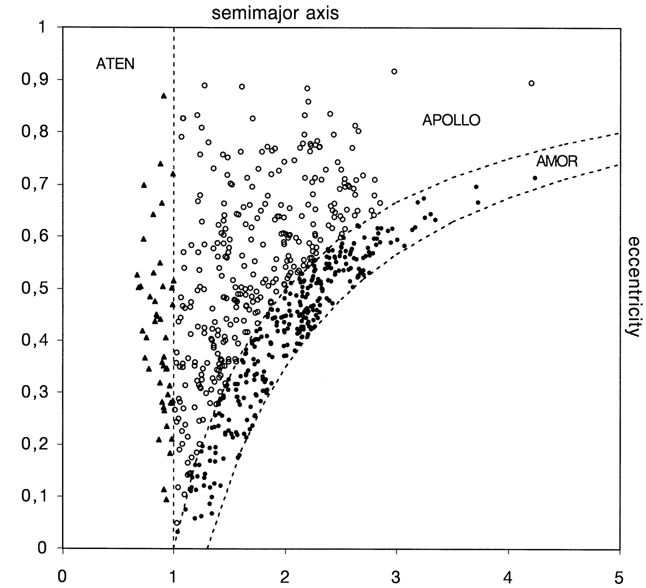

Fig. 2. Distribution of NEAs in the a–e plane. Triangles are used for the ATENs, open circles for the APOLLOs and full circles for the AMORs. A vertical dashed line has been drawn at 1 AU, while the other two curves mark the tangency condition to the orbit of the Earth separating the APOLLO and AMOR classes, and the upper limit ($q = 1.3$ AU) imposed to the AMORs perihelia.

and indicated as possible parent bodies of the HED (Howardite–Eucrite–Diogenite) meteorites.

Near-Earth Asteroids are usually divided into three classes, depending upon their orbital characteristics: ATEN asteroids have a semimajor axis a less than that of the Earth and aphelia Q larger than Earth's perihelion distance ($a < 1$ AU, $Q > 0.983$ AU), APOLLO asteroids have a semimajor axis greater than that of the Earth and perihelia q inside the aphelion distance of the Earth ($a > 1$ AU, $q < 1.017$ AU), AMOR asteroids are those with perihelia approaching from outside the orbit of our planet ($a > 1$ AU, $1.017 < q < 1.3$ AU). The sample of NEAs at our disposal is that available at the Minor Planet Center web page, and adds-up to a grand total of 661 objects: 47 Atens, 311 Apollos and 303 Amors (updated on 1999 February 7). Their density distribution for increasing values of their semimajor axis is shown in Fig. 1.

A meaningful way of looking at the orbital characteristics of the NEAs population as a whole is shown in the plot of Fig. 2, which relates eccentricity and mean distance from the Sun. In this representation, the three populations are well separated by the tangency condition with the orbit of the Earth and by the upper limit imposed to their perihelia.

The distribution of perihelion and aphelion distances, and the corresponding frequency histograms, are reported in Figs. 3(a), (b) and 4(a), (b) respectively. It is worthwhile noting that while the cutoff in the upper q distribution (Fig. 3(b)) is a direct consequence of the Amor class definition, the one appearing on the lower tail of the NEAs aphelia ($Q < 1$, Fig. 4(b)) is possibly due to an observational bias; in fact the discovery of objects with heliocentric distance always less than that of the Earth along its orbit is extremely difficult because of the small elongations from the Sun involved (Boattini and Carusi, 1997).

The distribution of NEAs inclinations i, is displayed in Fig. 5(a). A few objects may reach 50° or more, while the frequency histogram of Fig. 5(b) indicates that more than half of them have $i > 10°$. As it will be discussed in more detail in the following sections, this poses severe constraints to mission profiles, especially as far as rendezvous missions are concerned. In fact, the orbital inclination is a crucial parameter in deciding the accessibility of a target since out-of plane manoeuvres are in general rather demanding in terms of energy changes. As an example, in order for NEAR to rendezvous Eros, an intermediate Earth swingby has been necessary for increasing by the required 10° the inclination of the spacecraft orbit (Farquhar et al., 1995).

Another way of representing the dynamical characteristics of the NEAs population is to exploit the Tisserand parameter T_E and its significance in describing different orbital regimes. Indicating with a, e, i the asteroid's orbital elements and with a_E the semimajor axis of the Earth, we obtain

$$T_E = a_E/a + 2[a(1 - e^2)/a_E]^{1/2} \cos i. \quad (1)$$

This quantity is representative of the relative unperturbed velocity of the asteroid at close encounter with the Earth, as given by

$$U = (3 - T_E)^{1/2}. \quad (2)$$

If the negative value of the ratio of the semimajor axes $-a_E/a$ (a quantity related to the normalized asteroid orbital energy) is plotted against U^2 for every member of our sample, the plot reported in Fig. 6 is obtained. With respect to an a–e diagram such as that of Fig. 2, this plot provides a number of additional information. The curve on the left of

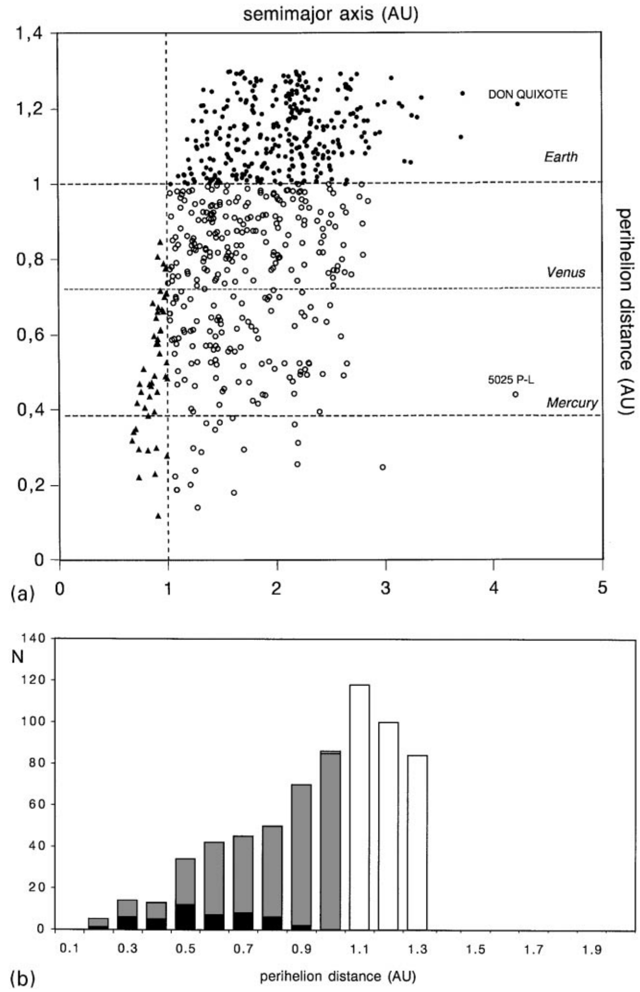

Fig. 3. (a) Distribution of the perihelia of the NEAs. Symbols are the same as in Fig. 2, while reference lines mark planetary distances. (b). Frequency histogram of the perihelia of the NEAs; the bin size is 0.1 AU.

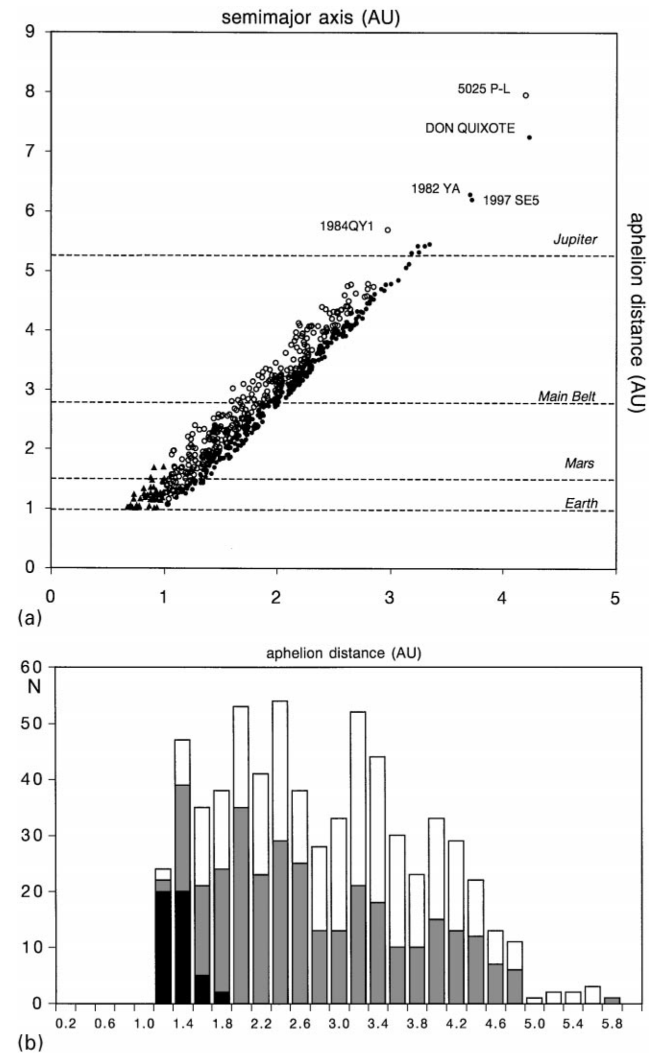

Fig. 4. (a) Same as Fig. 3a, for the aphelia of the NEAs. (b) Same as Fig. 3b, for the aphelia of the NEAs; the bin size is 0.2 AU.

the figure is obtained putting $i = 0$ and $e = 0$, thus representing the circular limit which bounds the forbidden region at its left ($e^2 < 0$). The Earth tangency condition is also plotted for $i = 0$, separating in the upper part of the figure the Amor and Apollo classes. In this representation main belt asteroids would fade into the Amor class starting from the upper left region of the figure. In the lower part, the cuspid drawn by the two previous curves and culminating in the position of the Earth (of coordinates: 0, -1) bounds the region where asteroids having an aphelion less or equal that of our planet should be found. In this representation, asteroids approaching the orbit of the Earth from inside would appear as the dynamical counterpart to the Amors, occupying a region opposite to them. The distribution of the Atens extends toward the rightmost side of the figure starting from the lower branch of the tangency condition curve. Finally, an additional reference line can be drawn which separates direct from retrograde motion, corresponding to 90° inclined orbits, i.e. those for which the z-component of the angular momentum vanishes (see Eq. (1)).

The distance along the x-axis of an object from the tangency condition gives an indication of the additional velocity required for accomplishing a basic rendezvous mission towards a given asteroid, which, as it will be explained in detail and quantitatively discussed in the following sections, aims to match the spacecraft energy and angular momentum with that of the target.

3. Transfer trajectories

The problem of finding the trajectory in space allowing a spacecraft to reach a given target can be solved in many different ways, depending on the level of approximation needed. Sophisticated optimal transfer algorithms, modelling not only the gravitational environment but also the

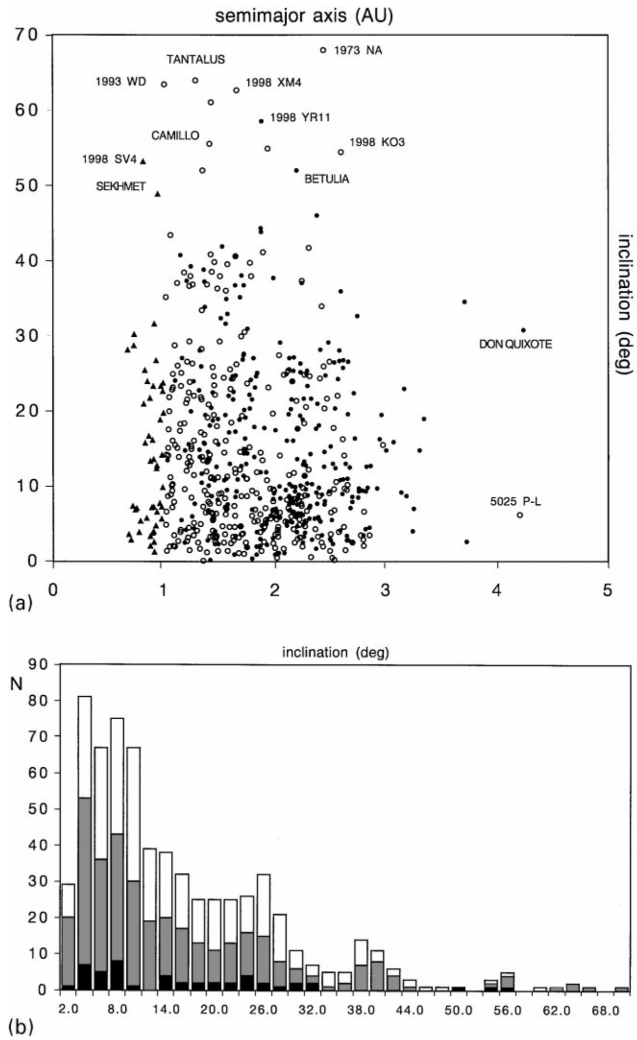

Fig. 5. (a) Same as Fig. 3a, for the inclinations of the NEAs. (b) Same as Fig. 3b for the inclinations of the NEAs; the bin size is 2°.

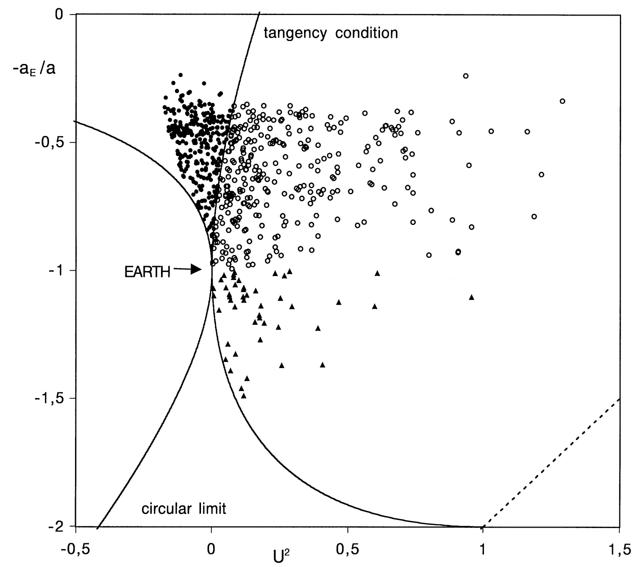

Fig. 6. Distribution of the NEAs in the (U^2, $-a_E/a$) space. Symbols are the same as in Fig. 2. The two curves represent the circular limit and the Earth tangency condition. The dashed line drawn at the bottom right corner of the figure corresponds to 90° inclined orbits.

navigation and propulsion systems on board the spacecraft, are used for operational purposes. In general, being based on minimization procedures, they are not easy to use and the solutions found may still be improved. For the purpose of this paper, namely to give a quick reference on the accessibility of NEAs, the approach based on Keplerian motion will suffice. In particular, the Hohmann transfer trajectories (e.g. Roy, 1988), giving the minimum energy transfer orbit parameters, and the Lambert problem (e.g. Pitkin, 1968), finding the trajectory joining two points in space for a given flight time, will be used.

The classical Hohmann transfer strategy provides the basic scenario for moving between two circular orbits around a central body: its rather simple formulation allows to estimate the delta-V (ΔV the velocity increment to be applied to an already free-flying spacecraft) needed for flyby and rendezvous missions with the planets or, changing the gravitational environment, for inserting an artificial satellite into a geostationary orbit around the Earth. The transfer is carried out in two different phases: an "apocentre raising manoeuvre" sizes the transfer trajectory in order to be tangential to the target orbit, while a subsequent "pericentre raising" takes place at the apocentre of the transfer trajectory in order to circularize the motion and reach the final orbit. This is done through well-known equations (e.g. Larson and Wertz, 1996) which exploit the interrelations among the shape and size of an orbit and the velocity vector:

$$\Delta V_1 = \mu^{1/2}[(2/r_1 - 1/a)^{1/2} - (1/r_1)^{1/2}], \qquad (3)$$

$$\Delta V_2 = \mu^{1/2}[(1/r_2)^{1/2} - (2/r_2 - 1/a)^{1/2}], \qquad (4)$$

where μ is the gravity parameter (since the mass of the spacecraft is negligible its value is given by the product of the gravitational constant times the mass of the central body), r_1 and r_2 are the radii of the initial and of the target orbit, respectively, and a is the semimajor axis of the transfer trajectory, which can be easily computed by the formula: $(r_1 + r_2) = 2a$.

If one applies this method continuously while assuming that the departure orbit is that of the Earth, it is possible to give a general picture of the energy requirements needed to access the inner and outer regions of the Solar System. A graphical representation can be obtained on a plane whose axes are the heliocentric distance and the absolute ΔV magnitude (in order to avoid negative values for transfers inside the orbit of the Earth). In doing so, $|\Delta V_1|$ gives the minimum value needed for reaching a given heliocentric distance, thus representing a flyby trajectory. The corresponding curve is the solid line reported in Fig. 7: it approaches at infinity the value of 12.34 km/s,

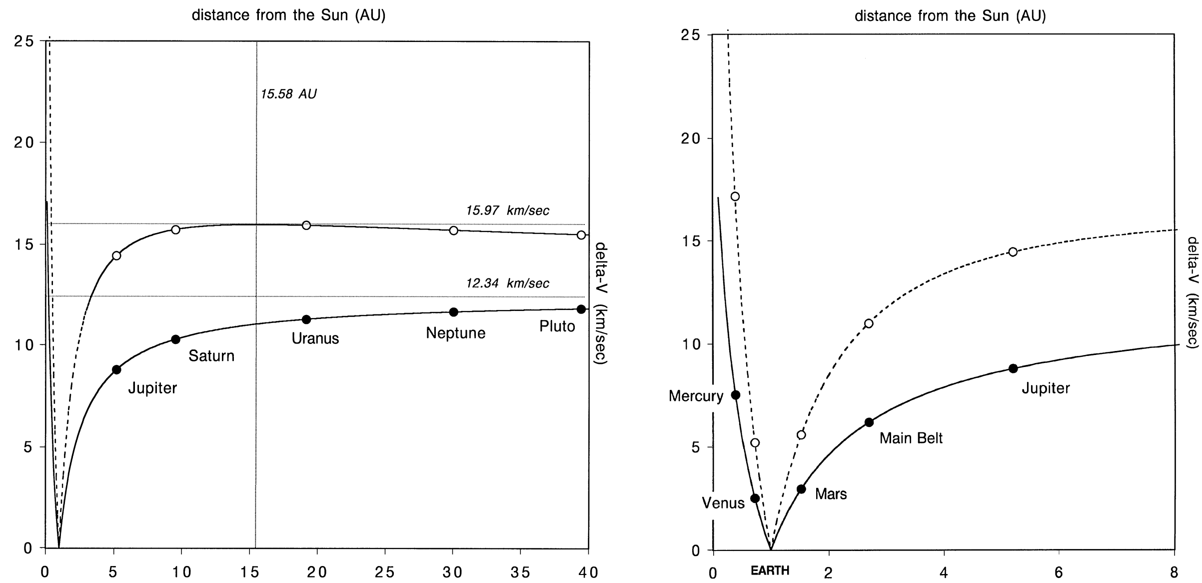

Fig. 7. Solar System H-plots on two different scales. Full circles give the ΔV needed to accomplish a Hohmann flyby trajectory toward the planets (assumed on circular coplanar orbits of radius equal to their actual mean distances from the Sun) and the asteroid main belt, while open circles show the additional ΔV required in order to circularize the corresponding transfer trajectories.

which is the escape velocity from the Solar System for a spacecraft initially moving along the orbit of the Earth (e.g. Gurzadyan, 1996). The sum $|(\Delta V_1 + \Delta V_2)|$ represents the total ΔV budget for a "planetary" rendezvous mission, which foresees also a manoeuvre to inject the spacecraft into a circular orbit of radius r_2. Its behavior, plotted in Fig. 7 using a dashed line, exhibits some peculiarities, as deduced by studying the function $|(\Delta V_1 + \Delta V_2)|$ and its derivative. For large heliocentric distances the curve tends toward the same limiting value as ΔV_1 but only after reaching a maximum of about 16 km/s at 15.58 AU. The location of this maximum turns out to have a strict dynamical interpretation: in fact, the Hohmann transfer represents an optimal strategy only if the ratio between the radius of the target and that of the departure orbits is less than 11.94. Exceeding this value the choice of a suitable bi-elliptic transfer is more convenient, while if $r_2/r_1 > 15.58$ *any* bi-elliptic transfer is favourable in terms of ΔV expenditure (e.g. Roy, 1988). Note that the bi-elliptic transfer is a three-impulse strategy which foresees an intermediate orbit with an apocenter distance larger than the target orbit, and this implies long transfer times, thus making it of almost no use for practical purposes.

This graphical representation, hereinafter called *H-plot*, provides a proper reference frame for discussing interplanetary trajectories. The distance along the y-axis between the two curves represents the ΔV difference between basic flyby and rendezvous missions. The location of the planets and the asteroid main belt is also remarked in Fig. 7 using open and full circles, allowing for example to visualize immediately the difficulties involved in reaching Mercury — which, incidentally, was the last terrestrial planet visited by a spacecraft. On the contrary, the outer planets are not much different in terms of ΔV requirements, being mainly characterized by the increasingly long flight time needed by the corresponding transfer trajectories.

The H-plot can also be exploited to represent more complex situations. As an example, the effect of non-zero orbital inclinations of the targets can be accounted for through the additional ΔV needed for a plane change. Combining the pericentre raising/lowering and the inclination manoeuvre, Eq. (4) can be rewritten as (Larson and Wertz, 1996)

$$\Delta V_2 = (V_\mathrm{i}^2 + V_\mathrm{f}^2 - 2V_\mathrm{i}V_\mathrm{f} \cos i)^{1/2}, \tag{5}$$

where V_i and V_f are the magnitudes of the osculating velocity vector at the beginning (e.g. at the apocentre of the transfer trajectory) and at the end of the manouvre, respectively, while i is the target inclination. The consequent increase of the total ΔV results in an upward drift from the corresponding reference line in the H-plot.

The approach described so far, does not take into consideration the phasing problem, that is the relative positions of the Earth and of the target object on their orbit at launch, which may not satisfy the Hohmann transfer geometry. This additional constraint poses strict time limitations for the actual encounter of the spacecraft with the desired target to occur and it is closely connected to the determination of the launch windows (e.g. in the case of NEAR, see Farquhar et al., 1995). Earth phasing is a rather sensitive parameter and plays a crucial role in determining the feasibility of a specific mission; nevertheless, our purpose is to define a general framework for the selection of NEAs targets which are both appealing from a scientific point of view and in principle technologically accessible, thus representing the first step towards more refined (and lengthy) mission analysis.

4. Rendezvous missions

The possibility of inserting a spacecraft in orbit around a small body has obvious advantages for science: close observations extended in time would allow detailed investigation on the composition and the morphology of its surface, on the shape of the object and on its rotational properties. Through the analysis of the spacecraft trajectory it is also possible to measure its mass and obtain indications on the internal structure. Furthermore, a rendezvous mission profile represents the first step toward a sample return strategy. From a mission analysis point of view this kind of mission is rather challenging if compared to simple flyby trajectories because it requires that the velocity vectors of the spacecraft and of the target, at encounter, be of equal magnitude and aligned.

In order to select possible NEAs targets for the ESA SMART-1 technology demonstration mission, Yanez et al. (1998) estimated the energy requirements for rendezvous missions computing the total ΔV needed to move a spacecraft from an initially 1 AU circular orbit into one identical in semimajor axis, eccentricity and inclination to that of the target. A similar approach has been applied to our NEAs sample exploiting the Hohmann transfer formalism. Depending upon whether an Aten, Apollo or Amor asteroid is targeted, the aphelion raising (Eq. (3)), perihelion raising or lowering and inclination change (Eqs. (4) and (5)) sequence of manoeuvres are rearranged in order to obtain the total ΔV expenditure. The H-plane can be then exploited for displaying the results and addressing the problem of the accessibility of the individual targets. In fact, if the aphelion distance of each asteroid is plotted on the x-axis a meaningful comparisons with the curves representing the classical Hohmann trajectories is possible. Should a NEA have an eccentric coplanar orbit tangent at perihelion or aphelion to that of the Earth, the corresponding point would be located along the solid line — its orbit being identical to the intermediate Hohmann transfer orbit described by Eq. (3). Thus, any displacement is a measure of the additional energy needed to lower (Aten and Apollo classes) or rise (Amors) the perihelia, as well as changing the inclination.

Fig. 8 shows the effect of NEAs eccentricities only (inclinations are neglected): the location of the Aten, Apollo and Amor classes is still recognizable and the larger displacements are found within the former two classes, which is a consequence of their definition. When also the effect of the inclinations is accounted for (Fig. 9) the three classes merge and there is a significant drift toward higher ΔV values, in many cases overcoming the limiting value for escaping the solar system. This is more apparent for objects of moderate eccentricity and small Q, which require the inclination manoeuvre to be performed within the inner solar system, where by Kepler's third law the velocity vector still keeps a significant magnitude (see also Fig. 7). The location of the dashed line, which represents the contribution for circularizing an Earth perihelion tangent orbit at any given aphelion distance (Eq. (4)), is well within the distribution of points; this suggests that in many cases a minimum energy rendezvous mission with an Earth approaching asteroid is far more demanding than

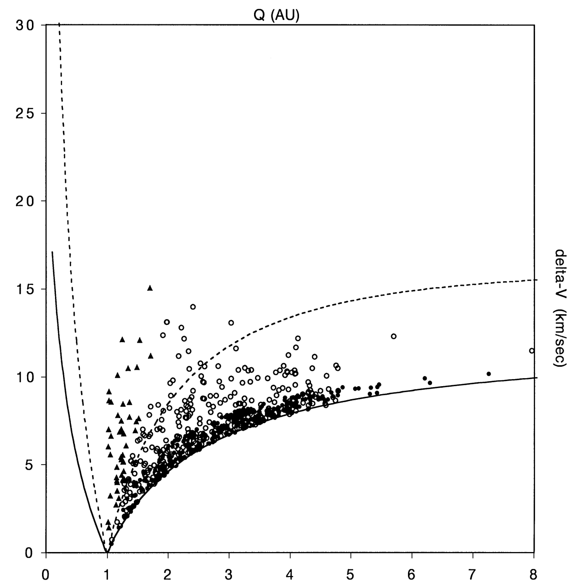

Fig. 8. H-plot distribution of NEAs when no inclination manoeuvres are taken into account. For each object, the ΔV corresponds to that needed to change an initially circular 1 AU orbit into a coplanar one having the same semimajor axis and eccentricity of that of the target asteroid.

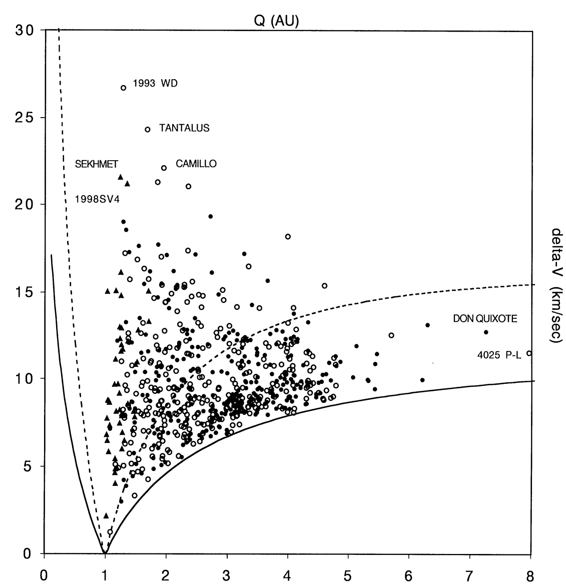

Fig. 9. H-plot distribution of NEAs when also the orbital inclinations are considered.

Table 1
Objects requiring a minimum ΔV for rendezvous. For each of them, perihelion (q) and aphelion (Q) distances, the inclination i, the absolute magnitude H and the minimum ΔV are listed

Name	q (AU)	Q (AU)	i (deg)	H	ΔV_{rv} (km/s)
1991 VG	0.977	1.077	1.4	28.5	1.26
1999 AO10	0.808	1.013	2.6	23.9	2.18
1996 XB27	1.119	1.257	2.5	22.0	3.00
1998 KY26	0.984	1.480	1.5	25.5	3.34
1998 HG49	1.065	1.335	4.2	22.0	3.88
1989 UQ	0.673	1.157	1.3	19.0	4.04
1998 KG3	1.024	1.298	5.5	22.5	4.23
1998 SF36	0.954	1.696	1.7	18.8	4.27
1989 ML	1.099	1.446	4.4	19.5	4.45
1998 RK15	1.246	1.589	0.2	22.0	4.61
1993 BX3	1.003	1.786	2.8	21.0	4.87

the equivalent Venus or Mars, and in some cases even Mercury or Jupiter, basic mission profiles.

Since a rendezvous mission calls for a nontrivial technical and financial support, most of the effort required during the preliminary studies is to try to maximize the superposition between “scientifically significant” and “technically feasible” targets. It is not always an easy task: as an example, the lowest ΔV objects appearing in the V-shaped bottom left corner of Fig. 9 are listed in Table 1. As it can be seen from their absolute magnitudes, they are all small-sized (diameter less than 1 km) thus, in general, not particularly attractive. On the other hand, finding a rigorous criterion to assess the scientific relevance of an asteroid, a rather subjective parameter, is also an elusive endeavour. Therefore, a search in the literature, exploiting extensively the NASA Astrophysics Data System web service, has been carried out: in order to isolate NEA members that can somehow ensure a “decent” scientific return, all objects mentioned at least once have been further investigated. Among them, those having a diameter less than 1 km and belonging to the rather common spectral S-type (such as Gaspra, Ida and Eros) have been discarded, unless possessing some peculiar properties (e.g. exotic rotation states, binary systems, etc.) Eventually, we ended up in isolating the set of 60 scientifically significant targets listed in Table 2. For each of them, the scientific motivations, and some relevant orbital parameters are reported. Studying the distribution of these selected objects in the H-plane appears then meaningful for the targeting problem.

Fig. 10 is an enlarged view of Fig. 9, where an upper limit to the available ΔV has been set (corresponding to the value for escaping the Solar System) and the location of the objects belonging to the selected asteroid sample of Table 2 is highlighted. The position of Eros within the plot witnesses a mission profile achievable using conventional propulsion and exploiting planetary swingby trajectories, while an overall budget of about 8 km/s was set during the study of the ESA SMART-1 asteroid option (Hechler et al., 1998), which foresees the use of solar electric propulsion. The chosen ΔV scale of Fig. 10 can thus be regarded as a sensible estimate of the present technological level.

Out of the 60 objects listed in Table 2, 44 appear also in the plot of Fig. 10. Among well-known NEAs, 4660 Nereus and 3361 Orpheus exhibit the lowest ΔV values. As a matter of fact, both turn out to be the best candidates for direct exploration: the former for the Japanese MUSES-C probe (Kawaguchi et al., 1996), while the latter for the ESA SMART-1 when more refined mission profiles, using a low-thrust optimization code, were computed (Hechler et al., 1998). However, the Japanese mission has been forced to change its target due to energy budget constraints (Yeomans, 1999), being now aimed towards 1989 ML, an object included in Table 1, whose accessibility can be also visualized in Fig. 10. A remarkably low ΔV is found in the case of 1998 KY26, a recently discovered asteroid that, notwithstanding its small dimension (40 m), has been indicated by Hicks et al. (1998) as peculiar because of its fast rotation.

Among the possible binary systems, asteroid 1991 VH (Pravec et al., 1998a) is located in the H-plane just below Eros. Its orbit is less eccentric and with a shorter period of revolution, although with a slightly higher inclination. Other interesting cases include the well-known potentially hazardous object 1997 XF11 (not too far from Eros in Fig. 10, having a larger aphelion but a smaller inclination), the highly elongated, fast rotating asteroid 1995 HM, and (3908) 1980 PA (recently named Nyx), a supposed fragment of Vesta-like bodies (Cruikshank et al., 1991).

Objects 6489 Golevka, 4179 Toutatis, and 4015 Wilson-Harrington can be regarded as both high-priority targets for science (see Table 2) and appealing from a dynamical point of view because of their low inclinations. Yet, although remaining close to the corresponding Hohmann transfer trajectories, they are located towards the rightmost region of the figure, indicating that most of the ΔV is spent to place the aphelion of the spacecraft orbit well beyond the asteroid main belt. This, together with the long revolution period (about 4 years), decreases the chances that a favourable mission opportunity is found within a given time span. As an example, in the case of asteroid 2063 Bacchus, whose ΔV requirement is comparable to that of the three aforementioned objects, a mission opportunity for SMART-1 was found in the period 2001–2004 (Hechler et al., 1998), while the search for suitable trajectories towards the other three NEAs, was unsuccessful.

5. Nodal flyby missions

Apart from representing an intermediate scenario, the main motivation for performing an asteroid flyby instead of a rendezvous is that the target requires a much too high

Table 2
scientifically relevant NEAs sample. For each object, the NEA class, the absolute magnitude (H), the diameter (D), the spectral type, the period of revolution (P), the aphelion distance (Q) and the orbital inclination (i) are listed. Remarks on the individual scientific relevance are also reported in the sixth column

Name	Class	H (mag)	D (km)	type	Remarks	P (yr)	Q (AU)	i (deg)
1989 VA	Aten	17.5	1.2	S	Fast rotator contact binary	0.62	1.162	28.8
(3753) Cruithne	Aten	15.1	—	—	Earth horseshoe	1.00	1.511	19.8
(3554) Amun	Aten	15.8	2.0	M	Metallic content fast rotator radar observations	0.96	1.247	23.4
(2100) Ra-Shalom	Aten	16.0	3.4	C (S)	Primitive main belt composition not easy to explain its present orbit radar observations	0.76	1.195	15.8
1998 KY26	Apollo	25.5	0.05	—	Monolythic fast rotator	1.37	1.480	1.5
1997 XF11	Apollo	17.0	—	C	Primitive main belt composition repeated near-future Earth close approaches	1.73	2.139	4.1
1997 BR	Apollo	17.5	—	—	Complex rotation state	1.54	1.744	17.2
1996 JA1	Apollo	21.0	—	—	Near-future Earth close approacher deep absorption bands at 0.9 micron radar observations	4.01	4.352	22.1
1991 VH	Apollo	16.5	1.0	E (M)	Double lightcurve binary	1.21	1.300	13.9
(Hermes) 1937 UB	Apollo	18.0		—	HED meteor parent body	2.01	2.662	6.1
(8201) 1994 AH2	Apollo	16.3	—	—	Cometary candidate	4.02	4.326	9.6
(7888) 1993 UC	Apollo	15.3	—	—	Fast rotator	3.80	4.052	26.0
(7753) 1988 XB	Apollo	18.6	—	—	HED meteor parent body	1.78	2.175	3.1
(7341) 1991 VK	Apollo	16.7	1.4	Q	Close connection with ordinary chondrites	2.51	2.776	5.4
(6611) 1993 VW	Apollo	16.5	1.9	Q	Close connection with ordinary chondrites	2.21	2.516	8.7
(5143) Heracles	Apollo	14.0	3.0	V	Possible Vesta fragment	2.48	3.250	9.1
(4769) Castalia	Apollo	16.9	1.4	—	Contact binary radar observations	1.10	1.577	8.9
(4660) Nereus	Apollo	18.2	0.7	C	To be visited by the MUSES-C spacecraft	1.82	2.026	1.4
(4197) 1982 TA	Apollo	14.6	2.8	S	Fast rotator contact binary close connection with ordinary chondrites	3.49	4.074	12.2
(4179) Toutatis	Apollo	15.3	3.2	S	Complex rotation state contact binary spectral hetereogenity: strong colour variations radar observations	3.98	4.104	0.5
(3361) Orpheus	Apollo	19.0	0.4	V	Possible Vesta fragment connection with basaltic acondritic meteorites	1.33	1.599	2.7
(3200) Phaethon	Apollo	14.6	6.9	F	Geminids meteors parent body strong cometary candidate	1.43	2.403	22.1
(3103) Eger	Apollo	15.4	1.5	E	Connection with enstatite achondrites/aubrites radar observations	1.67	1.904	20.9
(2212) Hephaistos	Apollo	13.9	5.7	SG	Strong cometary candidate	3.19	3.974	11.8
(2201) Oljato	Apollo	15.3	1.9	S	Strong cometary candidate radar observations	3.20	3.721	2.5
(2102) Tantalus	Apollo	16.2	—	—	Deep absorption bands at 0.9 ¯m	1.47	1.675	64.0
(2101) Adonis	Apollo	18.7	1.0	—	Strong cometary candidate orbit similar to comet P/Encke possible association with Taurid meteors falling into the Sun within some My	2.57	3.308	1.4
(2063) Bacchus	Apollo	17.1	2.0	C	It could have been (or will be) a Trojan asteroid radar observations	1.12	1.455	9.4
(1866) Sisyphus	Apollo	13.0	8.2	S	Fast rotator radar observations	2.61	2.914	41.2
(1865) Cerberus	Apollo	16.8	1.2	S	Highly elongated shape	1.12	1.585	16.1
(1864) Daedalus	Apollo	14.9	3.7	SQ	Close connection with ordinary chondrites	1.77	2.359	22.2
(1862) Apollo	Apollo	16.3	1.5	Q	Close connection with ordinary chondrites radar observations	1.78	2.295	6.4
(1685) Toro	Apollo	14.2	3.4	S	Resonant orbit at close encounters radar observations	1.60	1.963	9.4

Table 2 (*continued*)

Name	Class	H (mag)	D (km)	type	Remarks	P (yr)	Q (AU)	i (deg)
(1620) Geographos	Apollo	15.6	2.0	S	Highly elongated shape (tidally reshaped?) radar observations	1.39	1.663	13.3
(1566) Icarus	Apollo	16.9	1.5	S	Fast rotator radar observations	1.12	1.969	22.9
1998 PG	Amor	17.1	—	—	Double lightcurve binary	2.86	2.805	6.5
1995 HM	Amor	23.0	0.5	—	Fast rotator highly elongated shape	1.76	1.780	4.0
1994 AW1	Amor	17.5	—		Double lightcurve binary	1.16	1.188	24.1
(8034) 1992 LR	Amor	17.9	1.0	Q	Close connection with ordinary chondrites	2.48	2.579	2.0
(6489) Golevka	Amor	19.2	0.6	V	Possible Vesta fragment highly irregular body 3 : 1 resonance with Jupiter connection with basaltic achondritic meteorites radar observations	4.00	4.023	2.3
(6178) 1986 DA	Amor	15.1	2.3	M	Iron meteorites parent body radar observations	4.72	4.460	4.3
(6053) 1993 BW3	Amor	15.1	3.0	S	Fast rotator	3.15	3.283	21.6
(5751) Zao	Amor	14.8	6.3	S	Moderate size, almost spherical	3.05	2.992	16.1
(4954) Eric	Amor	12.6	10.8	S	Giant asteroid	2.83	2.899	17.5
(4055) Magellan	Amor	14.8	3.4	V	Possible Vesta fragment	2.46	2.414	23.2
(4015) WilsonHarrington	Amor	16.0	2.0	CF	Previously observed as an active comet strong cometary candidate	4.30	4.289	2.8
(3908) Nyx	Amor	17.4	1.0	V	Possible Vesta fragment radar observations past binary companion of asteroid Verenia?	2.67	2.809	2.2
(3691) 1982 FT	Amor	14.9	—	—	Complex rotation state	2.36	2.278	20.4
(3671) Dionysus	Amor	16.3	—	—	Double lightcurve binary	3.25	3.388	13.6
(3552) Don Quixote	Amor	13.0	19.0	D	Giant asteroid low-albedo primitive body strong cometary candidate	8.71	7.255	30.8
(3551) Verenia	Amor	16.8	0.9	V	Possible Vesta fragment past sungrazer past binary companion of asteroid 1980 PA?	3.03	3.112	9.5
(3352) McAuliffe	Amor	15.8	3.0	S	Parent body for ordinary chondrites former target for Deep Space 1	2.58	2.572	4.8
(3288) Seleucus	Amor	15.3	2.8	S	Complex rotation state	2.90	2.962	5.9
(3102) Krok	Amor	15.6	—	—	Very slow rotator (binary tidally evolved?)	3.16	3.116	8.4
(1917) Cuyo	Amor	13.9	5.7	—	Radar observations	3.15	3.235	23.9
(1627) Ivar	Amor	13.2	8.1	S	Radar observations	2.54	2.602	8.4
(1580) Betulia	Amor	14.5	5.8	C	Very high inclination radar observations	3.25	3.270	52.1
(1036) Ganymed	Amor	9.5	39.0	S	Largest giant NEA possibly a former member of the Maria family radar observations	4.33	4.090	26.6
(887) Alinda	Amor	13.8	—	—	Very slow rotator (binary tidally evolved?)	3.91	3.884	9.3
(433) Eros	Amor	11.2	22.0	S	Giant asteroid possibly a former member of the Maria family to be visited by the NEAR spacecraft radar observations	1.76	1.783	10.8

ΔV, which in the case of NEAs, as shown in Figs. 8 and 9, is mainly due to the high inclination of the orbit or, to a minor extent, when a high eccentricity causes a rather distant aphelion to occur.

If we constrain ourselves to simple fly-by mission profiles, NEAs are intrinsically accessible from Earth: their orbital characteristics indicate that at least one of their nodes may fall at an affordable heliocentric distance, whatever the orbital inclination. The fraction of the NEA population that can be reached exploiting simple fly-by nodal encounter trajectories depends therefore only upon the amount of hyperbolic excess velocity (V_{inf}) at our disposal, i.e. the additional velocity with respect to the Earth escape velocity with which an interplanetary trajectory is achieved.

In exploring the trajectories joining the Earth and a given position in space in the planar case solving Lambert's problem, Perozzi and Fabiani (1998) have shown

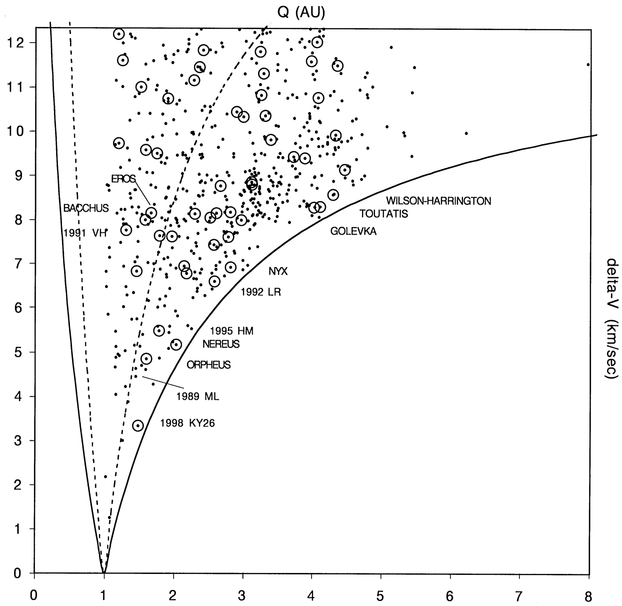

Fig. 10. Enlarged view of Fig. 9, setting an upper limit to the rendezvous ΔV equal to the solar system escape velocity. The location of objects belonging to the scientifically relevant sample listed in Table 2 is highlighted with an open circle; in a few cases asteroid names are also indicated.

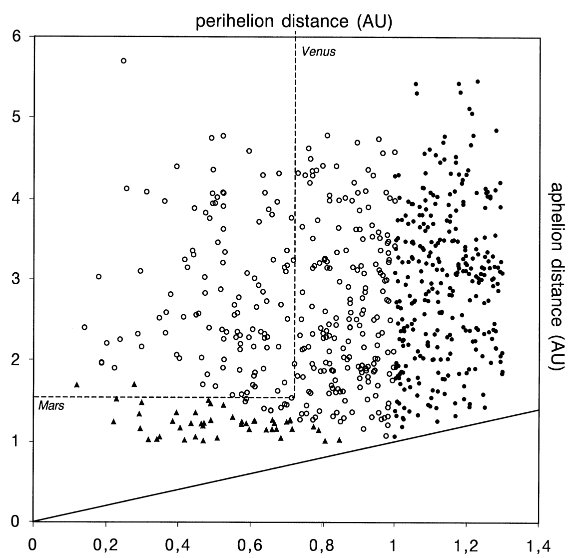

Fig. 11. Perihelia vs. aphelia relative distribution within the NEA population. The inclined solid line at the bottom of the figure marks the circular limit. Dotted lines corresponding to the Mars and Venus mean distances from the Sun isolate the region $\Delta V > 3\,\mathrm{km/s}$ described in the text.

that when no constraints are given to the flight time, a rather extended region surrounding the orbit of the Earth can be reached within realstic ΔV values. In particular, if a magnitude of 3 km/s is given to the maximum achievable V_{inf}, which appears a reasonable estimate for a small size mission allowing direct injection into interplanetary space, this region occupies a large portion of space between the orbits of Venus and Mars, provided that peculiar configurations are avoided.

In Fig. 11, the relationship among perihelia and aphelia of the NEA population is displayed. It shows that if the afore mentioned limit is assumed, only objects having at the same time perihelion distance smaller than the orbital radius of Venus and aphelion distance larger than that of Mars could be in principle out of reach, and then only when they satisfy the additional constraint of having apsidal lines lying close to the ecliptic. All other objects must have one of their nodes within the accessible region independently from the values assumed by the angular parameters. Nodal distances of NEA orbits have been then computed throughout the whole sample: those falling inside the selected 3 km/s region and corresponding to objects having either inclinations larger than 30° or aphelion distances greater than 4 AU have been listed in Tables 3 and 4,respectively. The energy requirements for nodal flybys (each object may offer two opportunities, corresponding to the ascending and descending nodes) have been computed and reported in the last column of these tables. A graphical representation of the distribution of NEAs nodal distances and of their inclinations is shown in Fig. 12, where the points corresponding to objects belonging to the selected NEA sample reported in Table 2 have been also highlighted. A comparison of this plot and Table 3 with Figs. 5(a) and 9 shows that, as expected, asteroids with aphelion distances not too far from 1 AU and very high inclinations, such as 1993 WD, Tantalus, Camillo and Sekhmet, which are very demanding for a rendezvous mission, could be in principle (i.e. only when an optimal Earth phasing also occurs) reached using simple flyby trajectories at less than 1 km/s. Among the scientifically relevant targets, Tantalus, Betulia, Sysyphus and Don Quixote exhibit the highest inclinations.

When considering the high aphelion objects listed in Table 4 the ΔV values needed for nodal encounters are generally higher, with the notable exception of the potentially dangerous bodies 1997 QK1, 1996 JA1, 1998 FW4, 1997 GL3, 1995 SA and 1998 DX11, having nodal distances within the Earth aphelion–perihelion range, thus encountering our planet at high relative velocities.

Asteroid 3552 Don Quixote, appearing both in Tables 3 and 4, is a primary target due to its large dimension and possible cometary origin. Only its rather distant ascending node falls inside the orbit of Mars (the other exceeding 4 AU), while its aphelion distance, by far the largest among the NEA sample, the high inclination and the long revolution period make it a rather difficult target to achieve.

Only five objects did not satisfy the nodal distance range taken into consideration for flyby missions: four Apollos (Heracles, Adonis, Hephaistos and Daedalus) and one Amor (Wilson-Harrington) — all included in the list of scientifically relevant targets. It is not surprising, from a dynamical point of view, that half of them are also strong cometary

Table 3
List of NEAs satisfying the constraints described in the text, sorted by inclination (i). For each object, the ascending (A) or descending (D) nodal distance (d) and the flyby ΔV_{fb} is reported. Asteroids belonging to the scientifically relevant sample of Table 2 are marked in bold type

Name	i (deg)	node	d (AU)	ΔV_{fb} (km/s)
(5496) 1973 NA	68.0	D	1.109	0.76
(2102) Tantalus	64.0	A	1.028	0.21
		D	1.369	2.24
1993 WD	63.5	D	0.793	1.77
		A	1.140	0.96
1998 XM4	62.7	A	1.124	0.86
1998 QH2	61.1	A	0.918	0.65
1998 YR11	58.6	A	1.135	0.93
(3752) Camillo	55.6	A	1.068	0.49
1997 MS	55.0	D	1.300	1.88
1998 KO3	54.5	A	0.880	0.97
		D	1.311	1.94
1998 SV4	53.3	D	1.340	2.09
(1580) Betulia	52.1	D	1.144	0.98
(5381) Sekhmet	49.0	D	1.131	0.90
1994 PN	46.1	D	1.274	1.74
1998 VP	43.9	D	1.356	2.17
1998 UL1	42.0	A	1.202	1.33
(1866) Sisyphus	41.2	A	1.109	0.76
1998 WT7	40.8	D	1.072	0.52
		A	1.216	1.42
(4257) Ubasti	40.7	A	1.199	1.32
		D	1.387	2.32
1999 AR7	40.6	A	1.410	2.43
1999 AN10	39.9	D	0.982	0.14
		A	1.015	0.11
(1981) Midas	39.8	D	1.000	0.00
		A	1.053	0.38
(8176) 1991 WA	39.6	A	1.327	2.02
1998 HM3	39.3	D	1.188	1.26
		A	1.301	1.89
1998 HJ41	38.9	D	1.263	1.68
		A	1.431	2.53
1996 FS1	38.6	A	1.335	2.07
1991 BB	38.5	A	0.903	0.77
		D	1.402	2.40
1992 BL2	38.1	A	1.325	2.01
1998 FF14	38.0	A	0.964	0.28
(8566) 1996 EN	38.0	D	0.983	0.13
1998 FF14	38.0	D	1.344	2.11
(5660) 1974 MA	38.0	A	1.372	2.25
1990 SA	37.8	D	1.359	2.19
1996 RY3	37.4	A	1.147	1.00
		D	1.231	1.50
(6455) 1992 HE	37.4	D	1.404	2.41
1996 AE2	37.3	A	1.111	0.77
		D	1.504	2.86
(7822) 1991 CS	37.1	D	1.032	0.24
		A	1.160	1.08
(4596) 1981 QB	37.1	D	1.372	2.25
(7889)1994 LX	36.9	A	0.829	1.43
1992 CC1	36.9	A	0.887	0.90
1997 YR10	36.8	D	1.151	1.03
(3553) Mera	36.8	A	1.338	2.08
1998 QQ	36.7	A	1.377	2.27
(9400) 1994 TW1	36.0	A	1.361	2.20
1998 UP1	35.2	D	0.746	2.26
		A	1.107	0.74
1998 SF35	35.2	D	1.448	2.61

Table 3 (*continued*)

Name	i (deg)	node	d (AU)	ΔV_{fb} (km/s)
(4957) Brucemurray	35.0	D	1.449	2.62
1982 YA	34.6	D	1.221	1.45
1998 MT24	34.0	D	1.178	1.20
1991 JG1	33.9	A	1.157	1.07
(7482) 1994 PC1	33.5	A	0.983	0.13
(3199) Nefertiti	33.0	A	1.237	1.54
1994 JX	32.7	D	1.163	1.10
1998 UN1	32.4	A	1.427	2.52
		D	1.453	2.63
1997 AC11	31.7	A	1.109	0.76
1998 XA5	31.7	D	1.118	0.82
1997 VG	31.0	D	1.077	0.55
(3552) Don Quixote	30.8	A	1.365	2.22
1996 XW1	30.6	D	1.313	1.95
		A	1.433	2.54
1998 SO	30.3	D	1.241	1.56

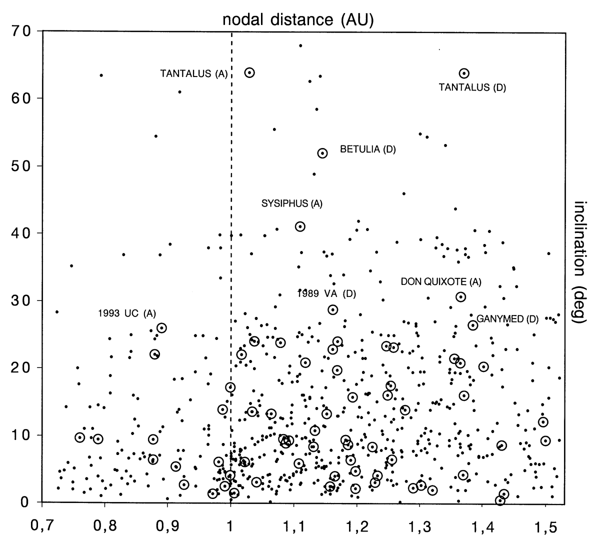

Fig. 12. Distribution of the NEAs nodal distances falling between the orbits of Venus and Mars plotted as a function of their orbital inclination. Open circles have the same meaning as in Fig. 10. The location of some asteroids is also indicated, with a further distinction between the ascending (A) and descending node (D). The grouping of low inclination objects close to 1 AU is possibly due to an observational bias.

candidates (see Table 2), thus having typical Short-Period comet orbits.

6. Resonant flyby missions

Although a nodal flyby mission may offer the only chance for encountering a given NEA, it has the disadvantage of lasting only a very short time if compared to the overall mission duration. Moreover, the encounter geometry and the relative velocity between the spacecraft and the target may not allow accurate observations, which are essential in order to support the funding of an

Table 4
Same as Table 3, for NEAs sorted by aphelion distance (Q)

Name	Q (AU)	Node	d (AU)	$\Delta V_{\rm fb}$ (km/s)
(3552) Don Quixote	7.255	A	1.365	2.22
1982 YA	6.291	D	1.221	1.45
1997 SE5	6.208	A	1.510	2.89
(5370) Taranis	5.461	D	1.253	1.63
1995 QN3	5.430	A	1.495	2.82
1997 YM3	5.427	A	1.485	2.78
1997 EN23	5.322	A	1.184	1.23
1998 GL10	5.309	A	1.474	2.73
1994 LW	5.123	A	1.436	2.55
1998 SE35	4.790	A	1.354	2.16
1998 FR11	4.788	D	0.838	1.34
(5324) Lyapunov	4.780	A	1.246	1.59
1998 VD31	4.780	A	1.377	2.28
1998 SY14	4.744	A	0.982	0.13
1998 MX5	4.704	A	1.357	2.18
1986 JK	4.701	D	1.065	0.46
1991 XB	4.676	D	1.214	1.40
1998 SH2	4.628	D	1.159	1.08
		A	1.493	2.81
1997 UZ10	4.621	A	1.095	0.67
1998 KO3	4.598	A	0.880	0.97
		D	1.311	1.94
1997 QK1	4.584	A	1.000	0.00
1995 DV1	4.573	A	1.379	2.28
1999 AF4	4.566	D	1.123	0.85
1985 WA	4.551	A	1.118	0.82
1994 AB1	4.530	A	1.189	1.26
1998 ST4	4.500	D	1.184	1.23
1983 LC	4.498	D	0.767	2.03
1987 QB	4.462	D	1.163	1.10
(6178) 1986 DA	4.460	D	1.369	2.24
1983 VA	4.415	A	0.808	1.63
1998 US18	4.411	D	1.091	0.64
1995 SD1	4.370	D	1.207	1.36
1996 TP6	4.364	D	1.249	1.60
1996 SK	4.361	A	0.749	2.22
		D	1.094	0.66
1990 HA	4.359	A	0.926	0.58
1996 JA1	4.351	D	1.017	0.13
1998 WA2	4.327	D	1.284	1.80
(8201) 1994 AH2	4.325	A	0.760	2.11
1994 JX	4.325	D	1.163	1.10
1998 FW4	4.319	A	0.988	0.09
		D	1.436	2.56
1994 US	4.316	D	1.427	2.51
1998 QR15	4.310	A	1.408	2.43
1992 UY4	4.304	A	1.096	0.67
(7092) Cadmus	4.302	D	1.250	1.61
		A	1.306	1.92
6344 P-L	4.298	D	1.111	0.77
(3360) 1981 VA	4.296	A	0.810	1.61
1998 HT31	4.296	A	1.171	1.15
		D	1.475	2.73
(7236) 1987 PA	4.248	A	1.220	1.44
1996 XX14	4.209	D	0.888	0.90
1990 TG1	4.205	A	0.820	1.51
1998 RN1	4.149	A	1.294	1.85
1998 QA105	4.140	A	1.347	2.13
1998 QH28	4.103	A	1.245	1.58
(4179) Toutatis	4.103	A	1.428	2.52
1997 TC25	4.091	A	1.063	0.45
(1036) Ganymed	4.091	D	1.384	2.31
1998 QS52	4.090	A	0.964	0.27
1994 GY	4.089	D	1.259	1.66
(9400) 1994 TW1	4.088	A	1.361	2.20
1994 RB	4.084	A	1.057	0.41
1994 XD	4.079	D	0.867	1.08
(4197) 1982 TA	4.074	A	1.496	2.82
1997 GL3	4.071	D	0.775	1.95
		A	1.016	0.12
1995 LE	4.060	A	1.518	2.92
(7888) 1993 UC	4.052	A	0.890	0.88
(2059) Baboquivari	4.045	D	1.265	1.69
1997 XS2	4.045	A	1.301	1.89
(4401) Aditi	4.038	A	1.439	2.57
(6489) Golevka	4.024	A	1.290	1.83
1995 EK1	4.023	D	1.381	2.29
1995 SA	4.022	A	1.008	0.06
1998 DX11	4.018	D	1.004	0.03

interplanetary mission. As a matter of fact, main-belt and near-earth asteroid flybys are considered at present only as cruise science return of space missions having different primary targets, such as the Galileo and Cassini missions to Jupiter and Saturn or the more recent NEAR and Deep Space 1. Multiple asteroid tours have been often taken into consideration but were never realized, due to the intrinsic difficulties encountered. The NASA Contour discovery class mission, which plans to encounter three Short-Period Comets, namely P/Encke, P/D'Arrest and P/Schwassmann-Wachmann 2, makes extensive use of Earth swingby trajectories in order to reach its targets. Therefore, it appears worthwhile to explore a strategy capable of increasing the scientific return of a mission towards a single NEA target, without increasing dramatically its overall complexity nor its ΔV budget.

In the book by Bruce Murray (1989) *Journey Into Space* which reports the early pioneering years of the exploration of the Solar System, while describing the Mariner Venus Mercury (MVM) mission, it is read:

⟨⟨At about this time, MVM got another boast from the giant brain of Beppe Colombo. I barely knew this short, balding man, with one of the most engaging smiles in the world, when he showed up at an MVM science conference at Caltech in February 1970. Afterward he came up to speak to me. "Dr. Murray, Dr. Murray" - he said - "before I return to Italy, there is something I must ask you. What should be the orbital period of the spacecraft about the Sun after the Mercury encounter? Can the spacecraft be made to come back?⟩⟩

As it turned out, the orbital period of the spacecraft was remarkably close to the 1 : 2 mean motion resonance with Mercury, a fact that allowed (after a small manoeuvre, needed to match the exact resonant value) to perform repeated encounters with the planet, which occurred on March 29, September 21, 1974, and March 16, 1975 — once every two mercurian years. A similar idea was also discussed by Roy (1963) for orbits commensurate with the 1-year period of the Earth.

Thus, one may try to exploit orbital resonances also in the case of NEAs, synchronizing the post-encounter orbital period of the spacecraft to that of the target in order to allow repeated nodal flybys. The basic scenario for estimating the feasibility of a "resonant flyby" strategy can be obtained using again the coplanar Hohmann-transfer formalism. Once the trajectory needed to reach the asteroid node is achieved using Eq. (3), a post-encounter orbital manoeuvre is foreseen, whose aim is to increase (or decrease) the spacecraft semimajor axis until it matches the closest mean motion resonance with the target (Eq. (4)).

In the usual definition, a mean motion resonance occurs when the ratio between the mean motions n, or alternatively the period of revolutions T of the asteroid and of the spacecraft can be expressed as an integer fraction:

$$n'/n = T/T' = p/(p+q), \tag{6}$$

where primed quantities are referred to the lowest mean motion object. In our case, the ratio between the spacecraft transfer orbit mean motion and that of the target asteroid (or its reciprocal) should be evaluated. The result characterizes the orbital change needed to reach an exact resonant value and to evaluate the corresponding ΔV. This procedure has been carried out throughout our NEAs sample; since a spacecraft has a limited lifetime, of the order of several years, only low number resonances have been taken into consideration, i.e. $p = 1, 2$ and $q = 1, 2$.

It is worthwhile noting that these resonances are not related to those that may be found between the mean motion of an asteroid and that of the Earth (e.g. the so-called Toro protected orbits, as described by Milani and Baccili, 1998), just like the resonant motion of the MVM spacecraft with Mercury did not imply a commensurability between the Earth and that planet. The semimajor axis, and then the period of revolution, of the Hohmann transfer nodal flyby orbit used in our computations to start searching for resonant motion is determined only by the target nodal distance. Unless a NEA has an almost circular, coplanar orbit remarkably close to that of the Earth, asteroid nodes are widely dispersed by the angular parameters throughout the inner Solar System.

An estimate of the total ΔV budget needed for resonant flyby missions towards a few significant NEA targets can be inferred from the data presented in Table 5. For each object, the ΔV required to reach a given mean motion resonance ($\Delta V_{\rm res}$) should be added to that characterizing the nodal flyby ($\Delta V_{\rm fb}$). According to Eq. (6), commensurabilities are rearranged in such a way that the asteroid's period of revolution is always unity: thus the time span between two subsequent encounters is obtained multiplying the target period (reported in the third column of Table 5) by the first argument of the chosen resonance. As an example, we consider the Aten asteroid 1989 VA (first line of Table 5), having a descending nodal distance slightly in excess of 1 AU. The best resonant configuration is achieved through the 2 : 1 resonance, with one encounter every two revolutions of the asteroid (1.24 yr), while the spacecraft completes only one. On the other hand, a 1 : 4 resonance would imply that encounters are separated by one revolution period of the asteroid, while the spacecraft runs four heliocentric orbits. Therefore, as the period of revolution of the target asteroid increases, less resonances can be exploited, being unrealistic to take into consideration subsequent encounters too distant in time

Asteroids are listed in Table 5 in order of increasing period. The more frequent occurrence of certain resonances within the different NEAs classes has a geometrical explanation, depending whether the spacecraft transfer orbit toward the node has a semimajor axis that exceeds that of the target or not. This determines if resonances reported on the left or on the right with respect to the 1 : 1 in Table 5 are preferred. Since the number of encounters within a given time span is also an important parameter for increasing the scientific return of a mission, low number commensurabilities with short period asteroids increase their frequency. By the same argument it follows that resonances nearby the one corresponding to the minimum ΔV should also be checked (e.g. see the case of asteroids Amun and Geographos in Table 5).

An overall picture of the opportunities found is obtained through the use of the H-plot of Fig. 13. Simple nodal-encounter trajectories, such as those described in the previous section, lie by definition along the lower solid line: thus any upward displacement of an object gives a quantitative indication of the additional energy needed to reach a resonant configuration. Two NEAs subsamples have been plotted in Fig. 13: to a background distribution of objects having an inclination larger than 10° (black dots), has been superimposed that of the selected sample of Table 2 (open circles). In this way, low inclination objects, for which rendezvous strategies might prove feasible, are recognizable by lacking redundancy (i.e. the presence of a central dot). For each target, the ΔV displacement computed corresponds to the closest resonance. The proximity of an object to the solid line thus implies that the coplanar Hohmann transfer trajectory required for a nodal flyby was remarkably close to one of the mean motion resonances taken into consideration. From Fig. 13 it can be seen that for most high-inclination NEAs, a minimum-energy resonant flyby strategy can be achieved with a total ΔV less than 3 km/s.

When combining the information of Table 5 and Fig. 13, some resonant-flyby mission opportunities can be outlined. Among scientifically appealing targets, 1566 Icarus, 4769 Castalia and 1994 AW1 exploit the 1 : 1 resonance and their short period of revolution for allowing roughly one encounter per year at less than 1.5 km/s.

Table 5
Results from applying the resonant flyby strategy to some selected NEAs. In the left section of the table some characteristic quantities of each individual object are listed, while in the right section the ΔV needed to reach a resonant mean motion has been computed throughout all commensurabilities taken into consideration. The total ΔV budget is obtained adding up the basic nodal flyby requirement ΔV_{fb} to that corresponding to a chosen resonance (ΔV_{res}). The frequency of encounters is obtained multiplying the asteroid's period of revolution by the first argument of the resonance. Note that in some cases an asteroid may have both, ascending and descending nodal distances (d) leading to favourable configurations for resonant flybys

Name	Node	P	d	ΔV_{fb}	ΔV_{res}										
		yr	AU	km/s	1:4	1:3	1:2	2:3	3:4	1:1	4:3	3:2	2:1	3:1	4:1
1989 VA	D	0.62	1.16	1.09	—	—	—	—	19.22	8.94	3.71	2.10	1.01	4.12	5.74
(3753) Cruithne	D	1.00	1.17	1.13	—	—	16.09	7.65	5.45	1.37	1.55	2.52	4.50	6.57	7.68
(3554) Amun	A	0.96	0.70	2.74	23.24	13.35	5.64	2.00	0.79	1.68	3.60	4.27	5.67	7.18	8.00
(3554) Amun	D	0.96	1.25	1.59	—	—	—	10.01	7.29	2.53	0.74	1.81	3.98	6.22	7.42
(2100) Ra-Shalom	D	0.76	1.19	1.28	—	—	—	16.57	12.07	5.53	1.41	0.09	2.51	5.18	6.58
(4769) Castalia	A	1.10	1.09	0.61	—	—	10.43	4.76	3.04	0.28	2.75	3.58	5.30	7.12	8.10
(1566) Icarus	D	1.12	1.16	1.09	—	—	11.71	5.39	3.55	0.04	2.54	3.41	5.18	7.06	8.07
1994 AW1	A	1.16	1.04	0.27	—	22.55	8.08	3.31	1.81	1.15	3.40	4.16	5.73	7.42	8.33
1994 AW1	D	1.16	1.17	1.14	—	—	10.85	4.87	3.10	0.29	2.79	3.63	5.36	7.19	8.18
(1620) Geographos	A	1.39	1.06	0.46	—	14.76	5.24	1.32	0.05	2.49	4.44	5.11	6.49	7.98	8.79
(1620) Geographos	D	1.39	1.15	1.03	—	19.05	6.50	2.11	0.72	2.03	4.11	4.82	6.29	7.86	8.71
(3200) Phaethon	D	1.43	0.88	0.97	16.66	8.97	2.60	0.45	1.47	3.56	5.20	5.77	6.96	8.25	8.96
1997 BR	D	1.54	1.00	0.01	19.72	9.96	2.95	0.28	1.36	3.53	5.23	5.82	7.04	8.36	9.08
(2101) Adonis	D	2.57	1.79	3.96	—	16.32	3.37	0.41	1.59	3.91	5.65	6.25	7.48	8.78	9.49
1998 PG	D	2.86	1.26	1.65	7.62	2.74	1.69	3.88	4.63	6.16	7.37	7.79	8.67	9.63	10.16
(2212) Hephaistos	D	3.19	0.38	7.62	2.13	3.61	5.23	6.12	6.44	7.11	7.66	7.85	8.26	8.72	8.98
(2201) Oljato	A	3.20	1.16	1.06	4.21	0.51	3.09	4.93	5.57	6.88	7.92	8.29	9.06	9.90	10.37
(2201) Oljato	D	3.20	0.99	0.06	2.40	0.68	3.80	5.44	6.01	7.19	8.13	8.47	9.17	9.94	10.36
(1580) Betulia	D	3.25	1.14	0.98	3.82	0.24	3.26	5.06	5.68	6.97	7.99	8.35	9.11	9.94	10.39
(4179) Toutatis	A	3.98	1.43	2.52	3.85	0.09	3.49	5.30	5.92	7.20	8.21	8.57	9.32	10.13	10.58
(6489) Golevka	A	4.00	1.29	1.83	2.43	0.84	4.06	5.72	6.29	7.48	8.42	8.76	9.45	10.22	10.64
(1036) Ganymed	D	4.33	1.38	2.31	2.19	1.06	4.24	5.87	6.44	7.60	8.54	8.86	9.55	10.30	10.72

Longer period, large Q objects, have the disadvantage of having generally higher nodal flyby ΔV and lower encounter frequency, even if they are found remarkably close to a resonance (e.g. 4179 Toutatis and 6489 Golevka). As far as very high inclination objects are concerned, the best opportunity found is for 1580 Betulia ($i = 52^\circ$), to be encountered at its descending node once every 3 years with a ΔV slightly in excess of 1 km/s. Giant NEA 1036 Ganymed still requires more than 3 km/s and has a rather long period of revolution. Among the cometary candidates, 2201 Oljato and 3200 Phaeton appear reasonably accessible: the former displays a very low ΔV opportunity when encountered at its descending node, while for the latter a choice between the 1 : 2 and the 2 : 3 resonance is left open.

The level of confidence of these results is, of course, tightly connected with the approximations implied in using always minimum-energy Hohmann transfer profiles, thus neglecting the Earth phasing problem, as it will be discussed in detail in the last section of this paper.

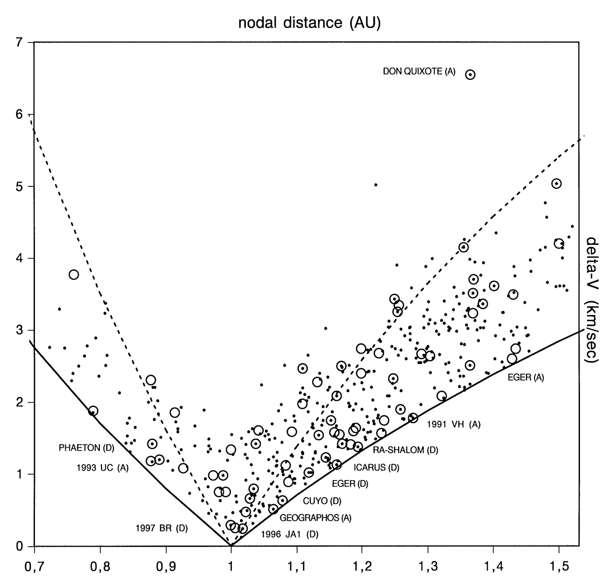

Fig. 13. H-plot of the resonant flyby strategy as described in the text.

7. Launch scenario

An important parameter influencing the feasibility of a mission is represented by the launch scenario, and in particular by the performances of the selected rocket, by its ability of supporting an upper stage, and by the existence and the technical characteristics of on-board propulsion systems. Whether the launcher is going to leave the spacecraft still within the gravitational field of our planet — thus needing an additional energy source to escape into interplanetary space — or deliver it directly on its deep space trajectory, this has an impact on the dimensioning of the payload and

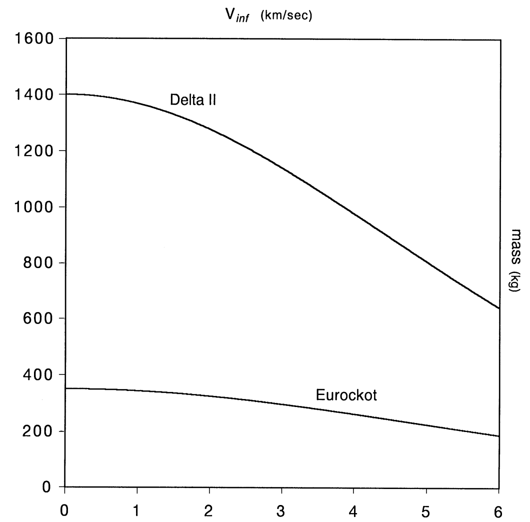

Fig. 14. Mass deliverable as a function of V_{inf} for the Eurockot and Delta II rockets.

on its cost. Therefore, converging towards a final launch configuration and mission profile cannot avoid interaction with the target selection process.

The world market of the space launches has definitely turn toward private companies offering launchers for the various needs of different space missions. With the current trend towards cheaper missions, the rocket may often represent the largest cost faced by a designer. Therefore the task of choosing the smallest possible launcher able to accomplish a desired mission becomes crucial. In the past years, several small launchers have been produced aimed mainly for launching small satellites into Low Earth Orbit (e.g. the airborne Pegasus rocket). They are capable of delivering only a few hundreds of kilograms into orbit at altitudes below 1000 km and therefore appear, at present, not suitable for launching even a small interplanetary probe. For this purpose a medium class launch vehicle has to be pursued. Without any aim of completeness (or advertising!), we will examine in some detail two of them: Eurockot and Delta II.

The Russian Eurockot, a modified SS-19 ICBM, was launched for the first time in 1994. As a standard performance, it is capable to deliver about 1800 kg in a circular Earth orbit around 300 km of altitude. It is the launcher proposed for the SMART-1 asteroid option; for this purpose it has been estimated (Hechler et al., 1998) that it could bring a mass of about 300 kg to escape the Earth gravitational attraction, with a hyperbolic excess velocity of about 2.83 km/s. Following Hechler et al. (1998), considering a value for the specific impulse (a measure of the exhaust velocity of the gas from the rocket nozzle) of 250 s, we can plot for Eurockot the mass deliverable at a given V_{inf} (Fig. 14). This last quantity is directly related to the ΔV_1 of Eq. (3), thus providing a first estimate of the feasible flyby missions. More complex missions can be accounted for through the so-called rocket equation:

$$\Delta V = gI_{\text{sp}} \ln(M_0/M),$$

where g is the gravity acceleration, I_{sp} is the specific impulse of the motor, M_0 and M are the initial and final spacecraft masses, respectively. Knowing the technical characteristics of the on-board propulsion system and the fuel mass, it is then possible to compute the ΔV available for further orbital changes, such as the pericentre raising or lowering manæuvre given by Eq. (4). Since, especially as far as rendezvous missions are concerned, fuel mass is a significant fraction of the total spacecraft (in the case of NEAR, it represented almost 50% of the total mass, while the science payload less than 10%) it is clear the role played by launchers in allowing more scientific experiments to be carried out.

A more powerful but consequently more expensive launcher is Delta II, the latest evolution of the Delta launch system, existing at present in various versions. On average, it is capable of delivering a few thousand kilograms into circular orbit around the Earth up to about 5000 km. For interplanetary injections the three-stage version — codenamed 7925 – should be used, adding a PAM-D rocket motor on top of the core vehicle. Delta II has already successfully launched several interplanetary missions: NEAR exploited a Delta II-7925-8, which is a version of the standard "off the shelf" rocket slightly modified to match the performances required by the mission, while Deep-Space 1 used for the first time a Delta 7326-9.5 Med-Lite. As shown in Fig. 14, Delta II exceeds by far the maximum performance of the Eurockot launcher: it could bring the 800 kg NEAR spacecraft to leave the Earth at a V_{inf} of about 5 km/s (nonetheless, as already pointed out, an Earth swing-by was needed in order to match the inclination of Eros). In comparison, the Eurockot launcher is barely sufficient to accomplish a small interplanetary mission.

A comparison of the performances of the Eurockot and Delta II rockets with the H-plot diagrams of Figs. 10 and 13 highlights the NEAs targets which might be accessible, following the corresponding basic mission profiles, with small and medium-size state-of-the-art launch systems. Moving to powerful launchers such as Atlas or Ariane is, of course, possible, but the cost of the mission would drastically grow.

8. Discussion and conclusions

The attempt of finding an overall accessibility criterion for Near-Earth Asteroids always requires some level of approximation in order to reduce the number of free parameters (the orbital characteristics of the target, Earth phasing, the total energy budget, the different mission profiles, the launch scenario, etc.). As an example, Lau and Hulkower (1987) introduced a measure of accessibility as the global minimum total ΔV for a two-impulse rendezvous mission profile (Hulkower et al., 1984). Notwithstanding the much smaller NEAs sample available at that time (82 objects) and the mission opportunities actually found within the period 1990–2010, no general rule could be stated. Therefore, in our approach we have tried on one side to reduce further the dynamical requirements, avoiding time-dependency and thus restricting to the "best case" basic transfer trajectories, while on the other side we account for the scientific relevance of the individual targets. Through the use of H-plots a general picture of the whole NEAs population has been presented, which allows to recognize the difficulties involved in specific cases and at the same time isolate those targets for which searching for more detailed mission profiles could be worthwhile trying. A summary of these results is presented in Table 6, where some relevant data for the three different mission profiles studied (rendezvous, nodal and resonant flybys) are listed for each member of the scientifically relevant NEAs sample considered. They can be grouped for discussion according to the most important topics that a space mission could help investigate.

Binary systems and/or contact binaries appear to occur rather frequently, as deduced from the shape of the lightcurves and radar observations. Among them, 4769 Castalia exhibits some favourable characteristics: although its rendezvous requirement is still high, its inclination is reasonably low, one of the nodes is remarkably close to 1 AU, while the period of revolution may lead to a 1 : 1 resonance trapping, thus allowing different mission scenarios to be investigated. Asteroid 4179 Toutatis, extensively imaged by radar and possibly in a peculiar rotation state, calls for a rendezvous mission: it has a negligible orbital inclination (0.5°), but the 4-year revolution period and the high eccentricity decrease the chances that a favourable opportunity is found. In the case of the high inclination Aten asteroid 1989 VA, a short revolution period and the location of its descending node could be exploited for frequent resonant flybys. Among the highly elongated objects, 1620 Geographos appears an opportunity worth investigating for different mission profiles, while 1995 HM exhibits one of the lowest rendezvous requirements.

The difficulties involved in trying to reach cometary candidates, because of their dynamical characteristics, have already been remarked. In the case of the shortest period object of this class, 3200 Phaeton ($P = 1.4$ years, $i = 22°$), a resonant flyby strategy could exploit the relatively low nodal flyby requirement and the 2 : 3 commensurability (total $\Delta V = 1.42$ km/s); the more convenient 1 : 2 resonance, can also be used, although at a higher price (total $\Delta V =$ 3.6 km/s, see Table 5).

V-type objects are also regarded as primary targets, because of their supposed origin as fragments of the basaltic surface of Vesta. Within this group the SMART-1 best target for rendezvous 3361 Orpheus is found, while for the others the situation is worsened by the distant aphelia, that in the case of 6489 Golevka may exceed 4 AU.

The potentially dangerous asteroid 1997 XF11, possibly a primitive C-type (Barucci and Lazzarin, 1999), has a moderate ΔV rendezvous requirement, together with 2063 Bacchus, belonging to the same spectroscopic type, which exhibits also a favourable 1 : 1 resonance.

The two asteroids indicated as having a high metallic content, 3554 Amun and 6178 1986 DA, are difficult to approach for opposite reasons. The former, an Aten, has an inclination of about 23°, mostly responsible for its high rendezvous ΔV; yet an interesting resonant strategy could be applied for frequent 1 : 1 resonant flybys (see also Table 5). The latter is a low inclination Amor type with a distant aphelion (4.5 AU): as a consequence it is less demanding for a rendezvous mission profile; on the other hand, efficient simple or resonant nodal flybys are prevented by the almost 5 years long revolution period and the rather far nodes.

Apart from 433 Eros, giant NEAs are not particularly accessible for rendezvous because of the high inclinations involved and the long revolution periods. In this respect 3552 Don Quixote, a 19 km sized cometary candidate and thus one of the most interesting NEAs to be visited by a spacecraft, is definitely the worst case with its almost 9 year period, 30° inclined orbit (see Figs. 3a, 4a, 5a); the consequences on its accessibility are clearly shown in Figs. 9, 12 and 13.

It should be, however, kept in mind that these considerations refer only to basic mission profiles: if, as an example, planetary swingbies are foreseen in the mission design process, even the most difficult cases may become feasible — depending only on complex but favourable dynamical configurations to be found. We are also aware that when Earth phasing is introduced for each specific object, even simple nodal flybys could become unfeasible for a very long period of time, as the farther a transfer trajectory is from the Hohmann type, the more sharply grows its ΔV requirement. For the same reason, resonant flyby opportunities should be computed starting from the actual transfer orbit found, which, in turn, might be close to resonances different from those presented here. Nevertheless, encouraging results have been obtained when searching for suitable candidates for the NEARER mission proposal (Perozzi et al., 2000), within the framework of the new Flexi-mission concept of the European Space Agency (ESA, 1999). Among the 24 scientifically significant targets that could in principle satisfy the rather stringent Flexi-mission constraints (e.g. nominal mission duration not longer than 2 years, reuse of already existing spacecraft, only low-cost medium-size launchers allowed, etc), four opportunities have been found, for launch dates within the time span 2005–2009, ensuring resonant encounters with the same NEA at a pace of about one flyby per year.

In conclusion, our aim was to give a general picture of the NEAs population from the point of view of mission analysis. Dedicated NEAs missions will surely take advantage of more refined trajectory design and of advanced propulsion systems in order to ensure the maximum return

Table 6
Summary of the ΔV requirements for rendezvous (ΔV_{rv}), simple nodal flyby (ΔV_{fb}) and resonant (ΔV_{tot}) strategies for the scientifically relevant NEAs sample of Table 2. Some orbital parameters and the closest resonance found (res) are listed

Name	P	ΔV_{rv}	Node	d	ΔV_{fb}	res	ΔV_{tot}	
1989 VA	0.622	15.1	A	0.295	9.67	3 : 4	10.44	ATEN
			D	1.161	1.09	2 : 1	2.09	
(3753) Cruithne	0.997	11.0	A	0.534	4.93	2 : 3	5.02	
			D	1.168	1.13	1 : 1	2.50	
(3554) Amun	0.961	11.6	A	0.701	2.74	3 : 4	3.53	
			D	1.247	1.59	4 : 3	2.33	
(2100) Ra-Shalom	0.759	9.7	A	0.469	5.99	3 : 4	6.82	
			D	1.193	1.28	3 : 2	1.38	
1998 KY26	1.367	3.3	A	1.434	2.55	1 : 1	2.74	APOLLO
			D	1.006	0.04	3 : 4	0.25	
1997 XF11	1.732	7.0	A	1.233	1.52	2 : 3	1.75	
			D	0.999	0.00	2 : 3	1.34	
1997 BR	1.542	9.5	A	1.534	2.99	1 : 1	3.81	
			D	0.999	0.01	2 : 3	0.29	
1996 JA1	4.098	11.5	A	1.839	4.12	1 : 2	6.05	
			D	1.017	0.13	1 : 4	0.24	
1991 VH	1.212	7.8	A	1.277	1.76	1 : 1	1.78	
			D	0.987	0.10	3 : 4	0.98	
(Hermes) 1937 UB	2.098	8.8	A	1.022	0.16	1 : 2	0.47	
			D	0.981	0.15	1 : 2	0.75	
(8201) 1994 AH2	4.019	9.9	A	0.760	2.11	1 : 4	3.77	
			D	3.520	7.39	3 : 4	9.06	
(7888) 1993 UC	3.800	12.0	A	0.890	0.88	1 : 4	1.20	
			D	2.898	6.54	3 : 4	7.07	
(7753) 1988 XB	1.779	6.8	A	1.041	0.30	2 : 3	1.61	
			D	1.229	1.49	2 : 3	1.57	
(7341) 1991 VK	2.502	7.6	A	2.756	6.30	1 : 1	6.64	
			D	0.913	0.69	1 : 3	1.86	
(6611) 1993 VW	2.207	8.1	A	1.186	1.24	1 : 2	1.60	
			D	1.430	2.53	2 : 3	3.49	
(5143) Heracles	2.482	10.8	A	1.567	3.12	2 : 3	4.44	
			D	0.482	5.76	1 : 4	5.98	
(4769) Castalia	1.096	8.0	A	1.087	0.61	1 : 1	0.89	
			D	0.652	3.32	2 : 3	3.56	
(4660) Nereus	1.817	5.2	A	1.945	4.45	1 : 1	4.64	
			D	0.972	0.21	1 : 2	0.98	
(4197) 1982 TA	3.486	10.8	A	1.496	2.82	1 : 3	5.04	
			D	0.674	3.06	1 : 4	4.15	
(4179) Toutatis	3.979	8.3	A	1.428	2.52	1 : 3	2.60	
			D	1.584	3.19	1 : 3	4.39	
(3361) Orpheus	1.329	4.8	A	0.926	0.58	3 : 4	1.08	
			D	1.303	1.90	1 : 1	2.64	
(3200) Phaethon	1.433	14.8	A	0.155	14.33	1 : 3	14.75	
			D	0.879	0.97	2 : 3	1.42	
(3103) Eger	1.667	10.7	A	1.364	2.21	3 : 4	2.51	
			D	1.118	0.82	2 : 3	1.02	
(2212) Hephaistos	3.190	11.6	A	2.482	5.78	3 : 4	6.25	
			D	0.383	7.62	1 : 4	9.75	
(2201) Oljato	3.201	9.4	A	1.157	1.06	1 : 3	1.58	
			D	0.991	0.06	1 : 3	0.75	
(2102) Tantalus	1.465	24.3	A	1.028	0.21	2 : 3	0.66	
			D	1.369	2.24	1 : 1	3.51	
(2101) Adonis	2.565	10.4	A	0.496	5.52	1 : 4	5.60	
			D	1.790	3.96	2 : 3	4.36	
(2063) Bacchus	1.119	6.8	A	0.789	1.81	3 : 4	1.88	
			D	1.182	1.22	1 : 1	1.41	
(1866) Sisyphus	2.605	15.1	A	1.109	0.76	1 : 2	2.47	
			D	1.701	3.64	2 : 3	4.70	
(1865) Cerberus	1.122	9.6	A	0.610	3.85	2 : 3	4.15	
			D	1.370	2.24	4 : 3	3.70	
(1864) Daedalus	1.766	11.5	A	0.603	3.95	1 : 2	5.59	
			D	1.842	4.13	1 : 1	4.58	

Table 6 (*continued*)

Name	P	ΔV_{rv}	Node	d	ΔV_{fb}	res	ΔV_{tot}	
(1862) Apollo	1.784	8.1	A	0.877	0.99	1 : 2	1.18	
			D	1.190	1.27	2 : 3	1.64	
(1685) Toro	1.598	7.6	A	1.500	2.84	1 : 1	4.20	
			D	0.877	0.99	1 : 2	2.31	
(1620) Geographos	1.391	8.2	A	1.064	0.46	3 : 4	0.51	
			D	1.152	1.03	3 : 4	1.75	
(1566) Icarus	1.119	14.4	A	0.200	12.60	1 : 2	13.60	
			D	1.161	1.09	1 : 1	1.13	
1998 PG	2.860	8.2	A	2.653	6.11	1 : 1	7.70	AMOR
			D	1.256	1.65	1 : 2	3.34	
1995 HM	1.764	5.5	A	1.721	3.71	1 : 1	4.82	
			D	1.165	1.11	2 : 3	1.55	
1994 AW1	1.162	12.2	A	1.037	0.27	1 : 1	1.42	
			D	1.169	1.14	1 : 1	1.42	
(8034) 1992 LR	2.478	6.6	A	1.321	1.99	1 : 2	2.09	
			D	1.803	4.00	2 : 3	4.05	
(6489) Golevka	3.996	8.3	A	1.290	1.83	1 : 3	2.67	
			D	2.167	5.06	1 : 2	5.09	
(6178) 1986 DA	4.720	9.1	A	2.857	6.47	1 : 2	8.17	
			D	1.369	2.24	1 : 4	3.23	
(6053) 1993 BW3	3.146	11.3	A	1.355	2.16	1 : 2	4.15	
			D	1.801	3.99	1 : 2	4.60	
(5751) Zao	3.050	10.3	A	1.249	1.60	1 : 3	3.43	
			D	2.797	6.37	1 : 1	8.02	
(4954) Eric	2.831	10.4	A	1.254	1.63	1 : 2	3.25	
			D	2.207	5.16	3 : 4	5.66	
(4055) Magellan	2.455	11.8	A	2.302	5.38	1 : 1	6.94	
			D	1.258	1.65	1 : 2	1.90	
(4015) Wilson-Harrington	4.299	8.6	A	1.639	3.41	1 : 3	4.05	
			D	1.604	3.27	1 : 3	3.68	
(3908) Nyx	2.673	6.9	A	2.080	4.83	3 : 4	5.36	
			D	1.198	1.31	1 : 2	2.74	
(3691) 1982 FT	2.363	11.2	A	1.952	4.47	3 : 4	4.60	
			D	1.401	2.39	1 : 2	3.61	
(3671) Dionysus	3.254	9.8	A	3.080	6.81	1 : 1	8.05	
			D	1.034	0.25	1 : 3	0.79	
(3552) Don Quixote	8.709	12.8	A	1.365	2.22	1 : 4	6.55	
			D	4.320	8.17	1 : 2	8.22	
(3551) Verenia	3.028	8.9	A	3.037	6.75	1 : 1	7.38	
			D	1.083	0.59	1 : 3	1.12	
(3352) McAuliffe	2.576	7.4	A	1.198	1.31	1 : 2	2.40	
			D	2.517	5.85	1 : 1	6.95	
(3288) Seleucus	2.897	8.0	A	1.108	0.75	1 : 3	1.98	
			D	2.919	6.57	1 : 1	7.20	
(3102) Krok	3.157	8.8	A	2.886	6.52	1 : 1	8.17	
			D	1.225	1.47	1 : 3	2.68	
(1917) Cuyo	3.153	11.8	A	3.135	6.89	1 : 1	7.58	
			D	1.078	0.55	1 : 3	0.63	
(1627) Ivar	2.543	8.2	A	2.563	5.94	1 : 1	6.70	
			D	1.131	0.90	1 : 2	2.28	
(1580) Betulia	3.252	17.2	A	3.080	6.81	1 : 1	8.04	
			D	1.144	0.98	1 : 3	1.23	
(1036) Ganymed	4.333	12.5	A	2.959	6.63	2 : 3	7.06	
			D	1.384	2.31	1 : 3	3.36	
(887) Alinda	3.917	9.4	A	1.092	0.65	1 : 4	1.59	
			D	3.809	7.70	1 : 1	8.29	
(433) Eros	1.761	7.6	A	1.783	3.93	1 : 1	4.68	
			D	1.133	0.91	2 : 3	1.54	

for science, yet small satellite and launchers technology and the increasing possibilities of accessing interplanetary space not only by the major space agencies, the newly developed technology programs and the reduction of launch and hardware costs, could take advantage from a quick assessment of reachable NEAs targets. In this respect, asteroids having both nodes not too far from Earth's orbit, as displayed in Fig. 12, increase their accessibility: this is the case of Amun, Geographos, Oljato and 1994 AW1 — as shown in Table 6. This, together with the possibility of planning a NEA encounter as a midcourse or end-of-mission target may also contribute to increase the number of objects visited by a spacecraft, thus probing the diversity of the NEAs population.

The approach described so far can also be easily updated, as present and near-future NEAs observation will increase dramatically the number of known objects, while spectroscopic surveys and radar observations characterize more and more the scientific interest of the individual targets.

Acknowledgements

The authors would like to thank Paolo Farinella and Richard P. Binzel for the many suggestions during the SMART-1 NEAs selection phase, and Elisabetta Dotto for her useful comments on the early developments of this paper. The work of E.P. at the Observatoire de Paris is supported by the "Giuseppe Colombo Research Fellowship" of the European Space Agency.

References

Barucci, M.A., Doressoundiram, A., Dotto, E., Farinella, P., Fulchignoni, M., Milani, A., Paolicchi, P., Perozzi, E., Rossi, A., 1998. A rendezvous mission with an earth approaching asteroid: a scenario for SMART-1. Observatoire de Paris 9/4/98.

Barucci, M.A., Lazzarin, M., 1999. Private communication.

Benson, J.W., 1998. Near earth asteroid prospector: a private space exploration and resources assessment mission. Proceedings of the Workshop on Space Exploration and Resources Exploitation, ESA-WPP-151.

Binzel, R.P., Xu, S., Bus, S.J., Bowell, E., 1992. Origins for the near-earth asteroids. Science 257, 779–781.

Boattini, A., Carusi, A., 1997. Atens: importance among near-earth asteroids and search strategies. Vistas Astron. 41 (4), 527–541.

Cruikshank, D.P., Tholen, D.J., Bell, J.F., Hartmann, W.K., Brown, R.H., 1991. Three basaltic earth-approaching asteroids and the source of the basaltic meteorites. Icarus 89, 1–13.

ESA Call for Mission Proposals for two Flexi-Missions (F2 and F3), 1999. ESA Science web site.

Farinella, P., Froeschlé, Ch., Froeschl, Cl., Gonczi, R., Hahn, G., Morbidelli, A., Valsecchi, G.B., 1994. Asteroids falling into the Sun. Nature 371, 314–317.

Farquhar, R.W., 1995. Introduction: the near-earth asteroid (NEAR) mission. J. Astronaut. Sci. 43 (4), 345–351.

Farquhar, R.W., Dunham, D.W., McAdams, J.V., 1995. NEAR mission overview and trajectory design. J. Astronaut. Sci. 43 (4), 353–371.

Gaffey, M.J., Burbine, T.H., Binzel, R.P., 1993. Asteroid spectroscopy: progress and perspectives. Meteoritics 28, 161–187.

Gladman, B., Michel, P., Froeschlè, Ch., 1999. The near-earth object population, preprint.

Gurzadyan, G.A., 1996. Theory of Interplanetary Flights. Gordon and Breach Publishers, The Netherlands.

Hechler, M., Cano, J.L., Yanez, A., 1998. SMART-1 mission analysis: asteroid option. ESOC MAS WP 403.

Hicks, M.D., Weissmann, P.R., Rabinowitz, D.L., Chamberlin, A.B., Buratti, B.J., Lee, C.O., 1998. Close encounters: observations of the earth-crossing asteroids 1998 KY26 and 1998 ML14. American Astronomical Society DPS Meeting 30,1006.

Hudson, R.S., Ostro, S.J., Harris, A.W., 1997. Constraints on spin state and hapke parameters of asteroid 4769 castalia using lightcurves and a radar-derived shape model. Icarus 130, 165H.

Hulkower, N.D., Lau, C.O., Bender, D.F., 1984. Optimum two-impulse transfers for preliminary interplanetary trajectory design. J. Guidance 7 (4), 458–461.

Kawaguchi, J., Uesugi, T., Fujiwara, A., Matuso, H., 1996. The MUSES-C world's first sample and return mission from near-earth asteroid: Nereus. Acta Astronaut. 39, 15–23.

Kicza, M., Vorder Bruegge, R., 1995. NASA's discovery program. Acta Astronaut. 35 (Suppl.), 41–50.

Larson, W.J., Wertz, J.R. (Eds.), 1996. Space Mission, Analysis and Design, 2nd Edition. Kluwer Academic Publishers, Dordrecht, The Netherlands.

Lau, C.O., Hulkower, N.D., 1987. Accessibility of near-earth asteroids. J. Guidance 10 (3), 225–232.

Lupishko, D.F., Di Martino, M., 1998. Physical properties of near-earth asteroids. Planet. Space Sci. 46, 47–74.

Milani, A., Baccili, S., 1998. Dynamics of earth-crossing asteroids: the protected Toro orbits. Università di Pisa 4.54.1092, preprint.

Murray, B., 1989. Journey into Space. W.W. Norton & Company, New York, USA.

Ostro, S.J., et al., 1995. Radar images of asteroid 4179 Toutatis. Science 270, 80–83.

Perozzi, E., Fabiani, V., 1998. On targeting long-period and new comets for small satellite missions. Proceedings of the Workshop on Space Exploration and Resources Exploitation, ESA-WPP-151.

Perozzi, E., Rossi, A., Valsecchi, G.B., Barucci, M.A., Carusi, A., Casalino, L., Colasurdo, G., D'Abramo, G., Dotto, E., Fulchignoni, M., Lagerkvist, C-I., Milani, A., Rickman, H., 2000. NEARER: a proposal for an ESA Flexi-mission featuring resonant encounters with a near-earth asteroid. Presentation to the ESA/SSWG.

Pravec, P., Wolf, M., Sarounovà, L., 1998a. Lightcurves of 26 near-earth asteroids. Icarus 136, 124–153.

Pravec, P., Wolf, M., Sarounovà, L., 1998b. Occultation/eclipse events in binary asteroid 1991 VH. Icarus 133, 79–88.

Pitkin, E.T., 1968. A general solution to the lambert Problem. J. Astronaut. Sci. 270.

Rabinowitz, D.L., Gehrels, T., Scotti, J.V., et al., 1993. Evidence for a near-earth asteroid belt. Nature 363, 704–706.

Richardson, D.C., Bottke, W.F., Stanley, G.L., 1998. Tidal distortion and disruption of Earth-crossing asteroids. Icarus 134, 47–76.

Roy, A.E., 1963. On the use of interplanetary probe orbits of periods commensurate with one year. Astronaut. Acta 9, 31–46.

Roy, A.E., 1988. Orbital Motion. Adam-Hilger Ltd, Bristol.

SMART-1, Small Mission for Advanced Research in Technology. ESA/SPC(97) 37. October 1997.

Steel, D.I., McNaught, R.H., Garradd, G.J., Asher, D.J., Taylor, A.D., 1997. Near-earth asteroid 1995 HM: a highly-elongated monolith rotating under tension?. Planet. Space Sci. 45, 1091–1098.

Yanez, A., Hechler, M., Cano, J.L., 1998. SMART-1 asteroid option: selected asteroids. ESOC 1998/3/26.

Yeomans, D.K., 1999. MUSES-C: A Near Earth Asteroid lander and sample return mission. ACM99 Abstracts.

Zappalà, V., Cellino, A., Di Martino, M., Migliorini, F., Paolicchi, P., 1997. Maria's family: physical structure and possible implications for the origin of giant NEAs. Icarus 129, 1–20.